Cellular and Molecular Life Sciences (2022) 79:175
https://doi.org/10.1007/s00018-022-04167-8



ORIGINAL ARTICLE

# FKBP51 modulates hippocampal size and function in post-translational regulation of Parkin

Bin Qiu[2,7] · Zhaohui Zhong[3] · Shawn Righter[4] · Yuxue Xu[2] · Jun Wang[2] · Ran Deng[2] · Chao Wang[2] · Kent E. Williams[5] · Yao-ying Ma[6] · Gavriil Tsechpenakis[4] · Tiebing Liang[5] · Weidong Yong[1,2]

Received: 6 May 2021 / Revised: 20 January 2022 / Accepted: 22 January 2022 / Published online: 4 March 2022


## Abstract

FK506-binding protein 51 (encoded by *Fkpb51*, also known as *Fkbp5*) has been associated with stress-related mental illness. To investigate its function, we studied the morphological consequences of *Fkbp51* deletion. Artificial Intelligence-assisted morphological analysis revealed that male *Fkbp51* knock-out (KO) mice possess more elongated dentate gyrus (DG) but shorter hippocampal height in coronal sections when compared to WT. Primary cultured *Fkbp51* KO hippocampal neurons were shown to exhibit larger dendritic outgrowth than wild-type (WT) controls and pharmacological manipulation experiments suggest that this may occur through the regulation of microtubule-associated protein. Both in vitro primary culture and in vivo labeling support a role for FKBP51 in the regulation of microtubule-associated protein expression. Furthermore, *Fkbp51* KO hippocampi exhibited decreases in βIII-tubulin, MAP2, and Tau protein levels, but a greater than 2.5-fold increase in Parkin protein. Overexpression and knock-down FKBP51 demonstrated that FKBP51 negatively regulates Parkin in a dose-dependent and ubiquitin-mediated manner. These results indicate a potential novel post-translational regulatory mechanism of Parkin by FKBP51 and the significance of their interaction on disease onset.

### Graphical abstract

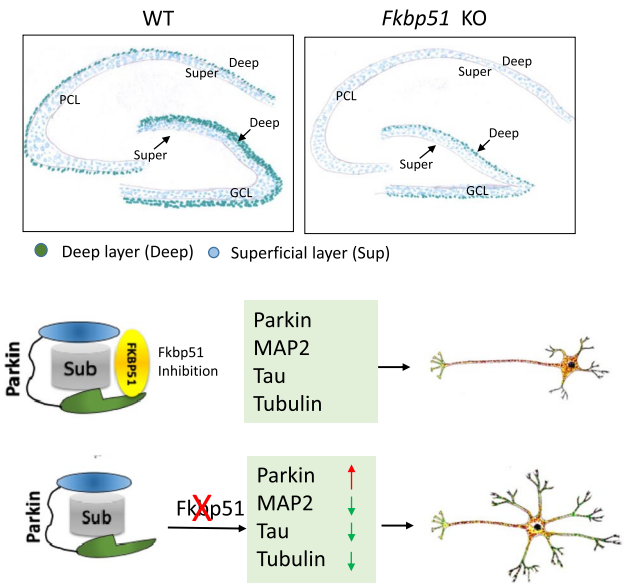


- KO has more flattened hippocampus using AI-assisted measurement
- Both pyramidal cell layer (PCL) of CA and granular cell layer (GCL) of DG distinguishable as two layers: deep cell layer and superficial layer. Distinct MAP2 expression between deep and superficial layer between KO and WT,
- Higher Parkin expression in KO brain
- Mechanism of FKBP51 inhibition resulting in Parkin, MAP2, Tau, and Tubulin expression differences between KO and WT mice, and resulting neurite outgrowth differences.

Bin Qiu and Zhaohui Zhong contributed equally to this work.

Extended author information available on the last page of the article

**Keywords** Fkbp51 · Hippocampus · Neuron · Parkin · Artificial intelligence

## Introduction

FK506-binding protein 51 (FKBP51, encoded by *Fkbp5*) belongs to a subclass of immunophilin proteins and has peptidyl-prolyl *cis–trans* isomerase (PPIase) activity that is crucial for protein folding [67]. One of the well-studied functions of FKBP51 is its role as a co-chaperone of heat shock protein 90 (Hsp90) in the formation of the glucocorticoid receptor (GR) complex, which is a central contributor to the stress response that modifies the pathophysiology of stress-induced conditions [70, 74, 76]. For example, *Fkbp51* has been associated with depression, post-traumatic stress disorder (PTSD), and other psychiatric disorders [21, 80, 84]. Newly emerging data indicate that FKBP51 may also play an important role in neuronal development, neurological diseases, and as a potential target for disease treatment [24, 40, 42, 51, 69, 79]. Interestingly, interactions with childhood adversity and emotion processing indicate that FKBP51 may play a role in neuronal plasticity through epigenetic regulation or an unknown function [1, 4, 25, 36].

The hippocampus is critical for learning and memory that experiences continuous neurogenesis into adulthood, and its volume has a relatively high level of heritability [34, 47, 64]. Hippocampal volume can be affected by neurogenesis or dendritic atrophy, which can be influenced by genetic predisposition, disease conditions, and certain therapies [29, 31, 38, 39]. Ample evidence supports the association between hippocampal volume and neurological and psychiatric diseases [53, 72, 77]. Significantly, FKBP51 has been associated with hippocampal volume alterations in PTSD patients [17, 38, 92]. The hippocampus is rich in corticosteroid receptors as well as FKBP51, and stress-induced glucocorticoid elevations result in many morphological and molecular changes in the hippocampus [14], 57. However, no study has been conducted using an *Fkbp51* knock-out (KO) model to directly assess its role in hippocampal morphology and disease development.

In this study, we examined the differences in hippocampal morphology between male *Fkbp51* KO and wild-type (WT) mice using an Artificial Intelligence (AI) approach, and determined the effects of *Fkbp51* ablation on neuronal development. Pharmacological manipulations were applied to understand the role of *Fkbp51* in microtubule dynamics. We measured the mRNA and protein levels of MAP2, Tubulin, Tau, and Parkin in *Fkbp51* KO and WT mice, and the functional relationships, particularly between FKBP51 and Parkin, were thoroughly investigated by knocking down and overexpressing *Fkbp51* in vitro. Co-immunoprecipitation (Co-IP) and co-transfection experiments support the role of FKBP51 in the regulation of Parkin. These findings suggest that *Fkbp51* plays a critical role in the dendritic complexity of neurons and is reflected by differences of deep cell layers of CA and DG between KO and WT in vivo, highlighting a potential mechanism underpinning differences in morphological, synaptic, and molecular function.

## Results

### *Fkbp51* gene deletion leads to altered hippocampal size

FKBP51 has been linked to hippocampal volume in human studies [38]. To directly confirm such an association, we examined if any changes in hippocampus morphology occur using the *Fkbp51* KO mouse model. Because the use of individual observers to define the morphological changes could be biased and limited, artificial intelligence (AI) tools were developed and applied to perform unbiased and in-depth surveys of the hippocampal area, using distinguishable cell layers, such as the neuron cell layers of *cornu ammonis* (CA) and the dentate gyrus (DG) as landmarks. Brain positions were registered and calibrated by the application of AI-assisted data analysis (Fig. 1A) and methods previously established by us and others [65, 78]. In brief, each image was preprocessed in grayscale with the locally adaptive histogram equalization method [95], followed by contrast enhancement and hybrid probability-driven deformable modeling [78]. The AI analysis suggested alterations in hippocampal size and DG size. Figure 1B depicts an overview of the results. The yellow region in the image is the segmentation outcome, while red lines are the resulting smooth centerlines along the interface, also shown in magnified views. Eight measurements were calculated for both left and right sides. The bar plots indicate corresponding measurements from all examined stacks across all depths. The results are shown in the numbered plots corresponding to the annotated measurements in the displayed magnified view (Fig. 1B). The cortex plus corpus callosum (CC) height was taller in KO than WT. Although the hippocampus height was found to be shorter in KO than WT, the length of the DG was found to be longer in KO than WT. The curve radii at CA1 was found to be larger in KO than WT, indicating more flattened curves. Interestingly, a genotype-specific left and right-side difference was found for CA3 curve radius, with opposing trends between KO and WT (Fig. 2B). These data demonstrate that the CA and DG of KO mice are significantly more elongated (horizontally) compared to WT, while the height of the hippocampus in KO is shorter (vertically). Our data

demonstrate the morphological consequences of knocking out *Fkbp51*.

### *Fkbp51* ablation affects neuronal development

A previous study demonstrated that FKBP51 plays a role in neurite outgrowth using cell lines and primary cultured hippocampal neurons from rats [59], but this role has not been directly studied using KO animal models. To uncover the effects of *Fkbp51* deletion on neuronal development and to identify its specificity, we examined the morphology of primary hippocampal neurons cultured from *Fkbp51* KO and WT mice. The neurons were immunofluorescence (IF)-labeled with βIII-tubulin, MAP2, and DAPI. At 3 days in vitro (*DIV*3), axonal specification and primary dendritic outgrowth had begun (Fig. 2). The distribution patterns of MAP2 and βIII-tubulin were similar between WT and *Fkbp51* KO neurons, but *Fkbp51* KO neurons exhibited lower MAP2 signal intensities (Fig. 2A, B, *DIV3* panel). At *DIV5* one long axonal outgrowth and few dendritic branches were clearly present in WT neurons. In *Fkbp51* KO neurons, one shorter axonal outgrowth and multiple overgrown dendritic branches were observed, an effect not evident in WT neurons (Fig. 2A, B. *DIV5* panel). Another striking difference was that KO cells had only weak labeling around the somatic and nuclear membranes, but WT cells had higher signal intensity for both βIII-tubulin and MAP2 labeling in these areas (Fig. 2, *DIV5*, magnified insets). Neuronal morphology differences were initially observed at *DIV3* but became more evident at *DIV*5 and *DIV*9 (Fig. 2). Quantitative data of MAP2 and βIII-tubulin are on the right of corresponding DIV panel (Fig. 2B). More representative neurons with different target labeling are shown in the Supplementary information (SI). Triple labeling of βIII-tubulin, F-actin, and DAPI (SI-Fig. 1A), or βIII-tubulin, Tau, and DAPI clearly shows more dendrite growth in KO (SI-Fig. 1A). Sholl analysis was performed to quantify observed differences using binary images created by *Image J* software (Fig. 2A. binary panel). Multiple neurons of each group were analyzed including primary branches (the number of branches that originated from the soma) and the radius of maximum intersections for the branches. The data indicate KO has a higher number of primary branches, increased radius (Fig. 2B), and more intersections at different radii (Fig. 2C), and with those measurements becoming more evident with increasing days in culture. These results suggest that knocking out *Fkbp51* has a significant impact on neuronal development, affecting the protein expression levels of microtubule-associated protein. This result is consistent with the role microtubule and actin dynamics play in determining neuronal polarization [90].

### Microtubule-stabilizing drug alters hippocampal neuron development in *Fkbp51* KO mice

Neurite outgrowth is essential for wiring the nervous system during development and in certain disease conditions [3]. We examined the involvement of FKBP51 in neuron development through the regulation of microtubules. Pharmacological interventions were applied to further investigate the function of FKBP51 in neurite outgrowth and its effect on microtubule dynamics during neuron development. In this experiment, a microtubule-stabilizing agent (Taxol, 3 nM) [37] or a microtubule-destabilizing agent (nocodazole, 50 nM) [11] was applied to *Fkbp51* KO and WT primary hippocampal neuron cultures. Similar to our previous observations, in untreated conditions, KO hippocampal neurite overgrowth was evident with βIII-tubulin and MAP2 labeling. MAP2 quantification between treatments is shown in Fig. 3B. As before, one long axon with a few short neurites were observed in WT neurons (Fig. 3A—vehicle panel). Following treatment with Taxol, the expression of MAP2 was affected in WT neurons (Fig. 3A, Taxol-WT panel), likely due to the ability of Taxol to promote microtubule stability and enhance protrusion of polymerizing dynamic microtubules to the growth cone. In *Fkbp51* KO neurons, the average total neurite number was higher than in WT after Taxol treatment (Fig. 3C), however, the intersections at radii close to the cell body were reduced to the level of WT neurons, with intersections with radii larger than 300 μm unaffected (Fig. 3D). Nocodazole treatment disturbed normal neuron morphology and produced neurite retraction in both KO and WT measured by radius (Fig. 3C, D). Sholl analysis indicated that KO possesses a higher number of primary branches and more intersections at different radii in the vehicle control and Taxol treatments when compared to WT. No differences between genotypes were observed with nocodazole treatment. The observation that Taxol affects dendrite overgrowth present in *Fkbp51* KO neurons suggests that the neuronal phenotype of the *Fkbp51* KO is associated with regulation of microtubule-related proteins.

### *Fkbp51* elimination affects tubulin, MAP2, and Tau protein expression

Cytoskeletal proteins, including microtubules, neurofilaments, and actin microfilaments, are important for maintaining neuronal morphology and function [27]. MAPs, particularly MAP2, Tau, and tubulin, are critical for neuron development and function. Given that dendrite outgrowth of cultured neurons was apparently affected by knocking out *Fkbp51*, we examined the in vivo mRNA and protein expression levels of MAP2 in the hippocampi of *Fkbp51* KO and WT mice. First, using quantitative real-time PCR, the levels of mRNA expression of *Tubb3* (encodes βIII-tubulin),

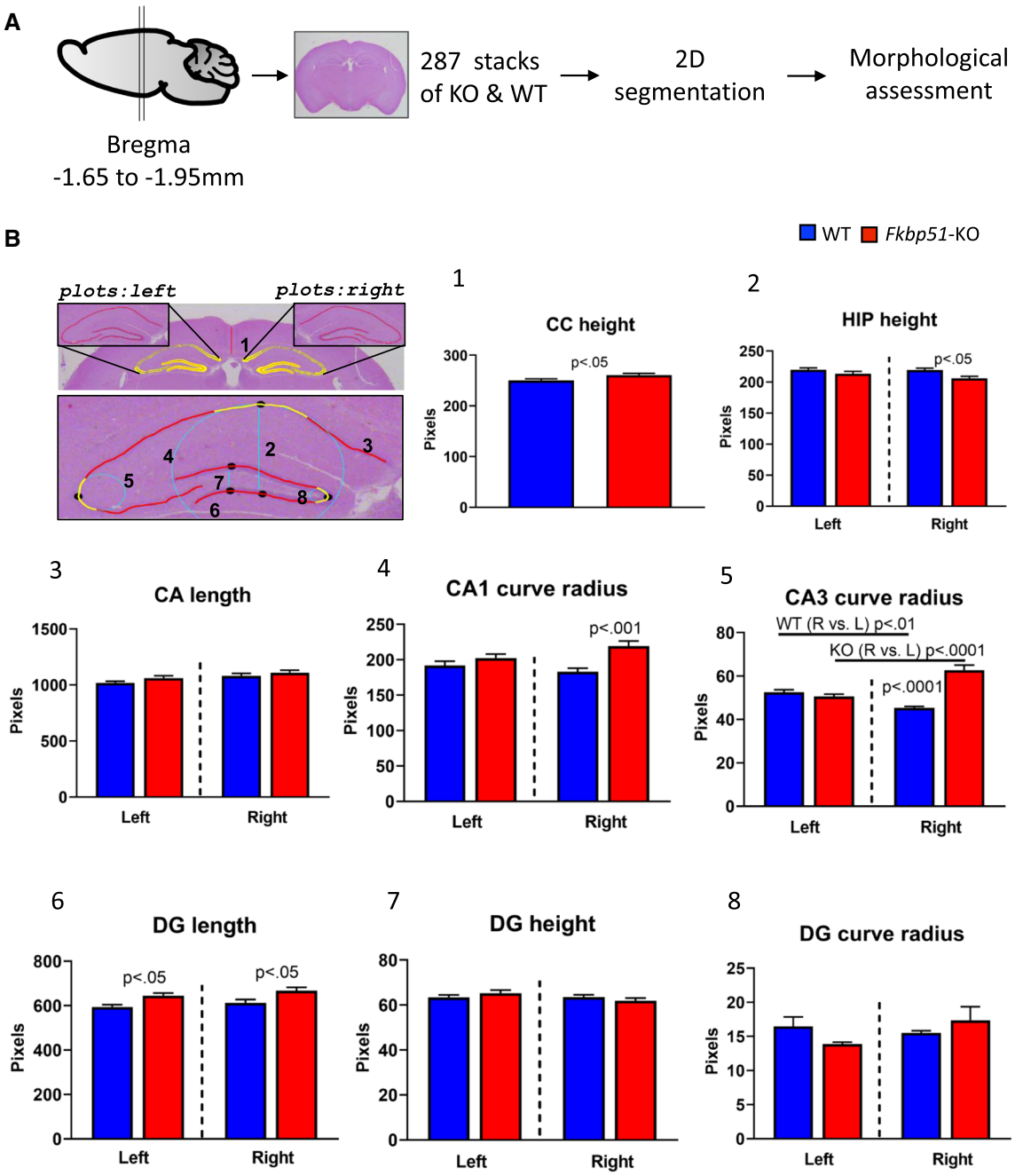


*Map2*, and *Tau* were determined. Unexpectedly, similar levels of mRNA expression were found between *Fkbp51* KO and WT mice (Fig. 4A). We then examined protein expression using βIII-tubulin, MAP2, and Tau IF labeling, immunohistochemical (IHC) labeling, and western blotting. In the DG, CA1, and CA3 subfields, significantly different expression patterns were found between KO and WT mice when observed in higher magnifications. In the DG, the granule cell layer (GCL), hilus region (HR), and molecular layer (ML) expressed lower levels of MAP2 in KO than in WT (Fig. 4B, DG panel). Notably, the deep layer (yellow arrow) of the GCL exhibited less intense labeling of MAP2 in *Fkbp51* KO mice than in WT mice and resulted in no visible labeling in this subfield. Similarly, low expression of MAP2 was observed in stratum oriens (Ori), pyramidal (Pyr) neuron layer, and stratum radiatum (Rad) of *Fkbp51* KO compared to WT, a pattern evident in the deep layer cell of the Pyr neuron layer of the CA1 and CA3 subregions (Fig. 4B). The differences in MAP2 expression in hippocampal deep layers and superficial layers indicate that neuronal development has been affected in KO mice.

◂**Fig. 1** Ablation of the *Fkbp51* gene compromises hippocampal size. **A** Image acquisition and data processing. Sagittal view with vertical lines indicating the position range where coronal sections were acquired. Stacks of images were analyzed from both 5 male WT and 5 male KO followed by 2D segmentation of areas of interest. Machine learning was applied and landmarks of CA and DG were analyzed. **B** Representative brain section with hippocampal subregions highlighted. The yellow regions indicate the 2D segmentation outcome, and red lines are the resulting smooth centerlines along the interface. Eight landmarks were measured, annotated in the magnified view at the bottom of the section (1) the cortex plus corpus callosum (CC) length was approximated using the vertical intensity profile of the contrast enhanced grayscale image; (2) the hippocampus height was calculated in the vertical direction, after the "peak point" between CA1 and CA2 was located; (3) the length of the hippocampus was calculated as the arc length of the pyramidal cell layer; (4) the local curve change at the "peak point" between CA1 and CA2 was captured by the radius of the best locally fit circle to the curve (in cyan); (5) similarly, the local curve change of CA3 was captured by the radius of the best locally fit circle; (6) the length of the colored DG segment was calculated as the arc lengths of the corresponding granular cell layer; (7) the DG height was measured vertically, after locating the peak point between the top and bottom granular cell layers; (8) the DG apex was captured by the radius of the best locally fit circle to the DG line. The y-axis in each plot corresponds to measurement in pixels, and the scale varies across the plots for illustration purposes. In blue and red are the measurements for WT and KO, respectively. The plots 2–8 are divided by a black vertical line into left and right hippocampus segment measurements. Bold dots indicate the group averages. CA: *cornu ammonis*. DG: dentate gyrus; Hippo: hippocampus. *P* value shown in (1) was determined by Student's unpaired t-test, shown in (2–8) were determined by One-way ANOVA

Furthermore, βIII-tubulin and MAP2 were co-labeled by IF. Lower levels of MAP2 expression were consistently observed in the DG and CA1 of KO mice, relative to those of WT mice (SI—Fig. 2, MAP2 panel). For βIII-tubulin, lower levels were also evident in the HR, GCL, and ML of the DG. Merged images display the labeling differences in the deep layers between KO and WT. The Pyr neurons at CA1 possessed significantly lower signal, evidence of deep cell layer differences in *Fkbp51* KO mice compared to WT mice (SI—Fig. 2, Merged panel. Particularly, greatly reduced labeling in the Rad layer, more pronounced in the alveus (Alv) and lacunosum-moleculare (LM) layers (SI—Fig. 2) was observed in the CA1 subregion of *Fkbp51* KO, signifying that FKBP51 affects neuronal tubulin.

The protein levels of MAP2, βIII-tubulin and Tau were further examined using IHC to gain cellular resolution. The extension of the neuronal dendritic tree into the Rad of CA1 and positively labeled cell number in the HR subfield of DG were investigated. For MAP2 labeling, KO mice showed less intensity than WT mice within the Pyr neuron cell layer, as well as in the apical branch in the Rad sub-region, which is consistent with what was observed in the cultured neurons (Fig. 4C—MAP2 panel). Similarly, βIII-tubulin and Tau had lower expression in the CA1 and HR of DG in KO mice, compared to WT mice (Fig. 4C). Quantitative IHC data can be found in SI—Fig. 4.

To gain a more quantitative understanding of the protein expression levels, western blotting was performed to quantify the total protein expression in the hippocampus, and results confirmed the low expression of these proteins including phosphorylated MAP2 in KO (Fig. 4D, E). Consistent with our in vitro primary neuron culture findings, in vivo βIII-tubulin, MAP2, and Tau labeling indicated clear differences in protein levels as well as sublayer expression differences in hippocampus between *Fkbp51* KO and WT mice. To determine if neurogenesis-driven differences in cell number contributed to the observed results, anti- Ki67 labeling was also performed. We found that in multiple subfields of the hippocampus, the total number of cell number counts as well as Ki67 positive cell counts between KO and WT showed no significant differences. The percentage of positive cells in total were also indicated (SI—Fig. 5).

## Increased Parkin levels occur in *Fkbp51* KO mice via post-translational regulation

Given the importance of Parkin in microtubule stabilization, we compared the expression of Parkin between *Fkbp51* KO and WT mice and assessed possible mechanisms of FKBP51 interplay with Parkin that could affect neuronal morphology. Strikingly, IHC labeling indicated clear differences in Parkin expression in hippocampal sublayers between *Fkbp51* KO and WT mice (Fig. 5A). The Pyr neurons at CA1 possessed significantly higher levels of Parkin in *Fkbp51* KO mice than in WT mice, with a stronger intensity of labeling in the Rad region. Similarly, higher expression of Parkin was observed in the GCL and HR in the DG of *Fkbp51* KO mice than in WT mice (Fig. 5A). Quantitative assessment revealed twice the level of Parkin protein in the hippocampal CA1 and DG area (Fig. 5A). In vitro IF labeling confirmed our in vivo observations. MAP2 and Parkin were co-expressed in cultured hippocampal neurons (*DIV*9) (Fig. 5B). As shown in the merged magnified image, the MAP2 signal is stronger, while Parkin is weaker in the soma of WT (Fig. 5Ba), MAP2 is much lower and Parkin is higher in the soma of *Fkbp51* KO (Fig. 5Bc). Magnification of the dendrites revealed that while Parkin is detectable in the WT neurons (Fig. 5Bb), in contrast, Parkin is highly expressed in *Fkbp51* KO dendrites (Fig. 5Bd). The observed punctate expression pattern of Parkin is similar to that described in previous reports [89]. Consistent with the IHC labeling results, western blotting revealed Parkin protein is significantly elevated in the *Fkbp51* KO hippocampus ($p < 0.001$) compared to WT hippocampus (Fig. 5C), although the lack of a difference in mRNA expression (Fig. 5D) suggested that Parkin could be post-translationally regulated by FKBP51.

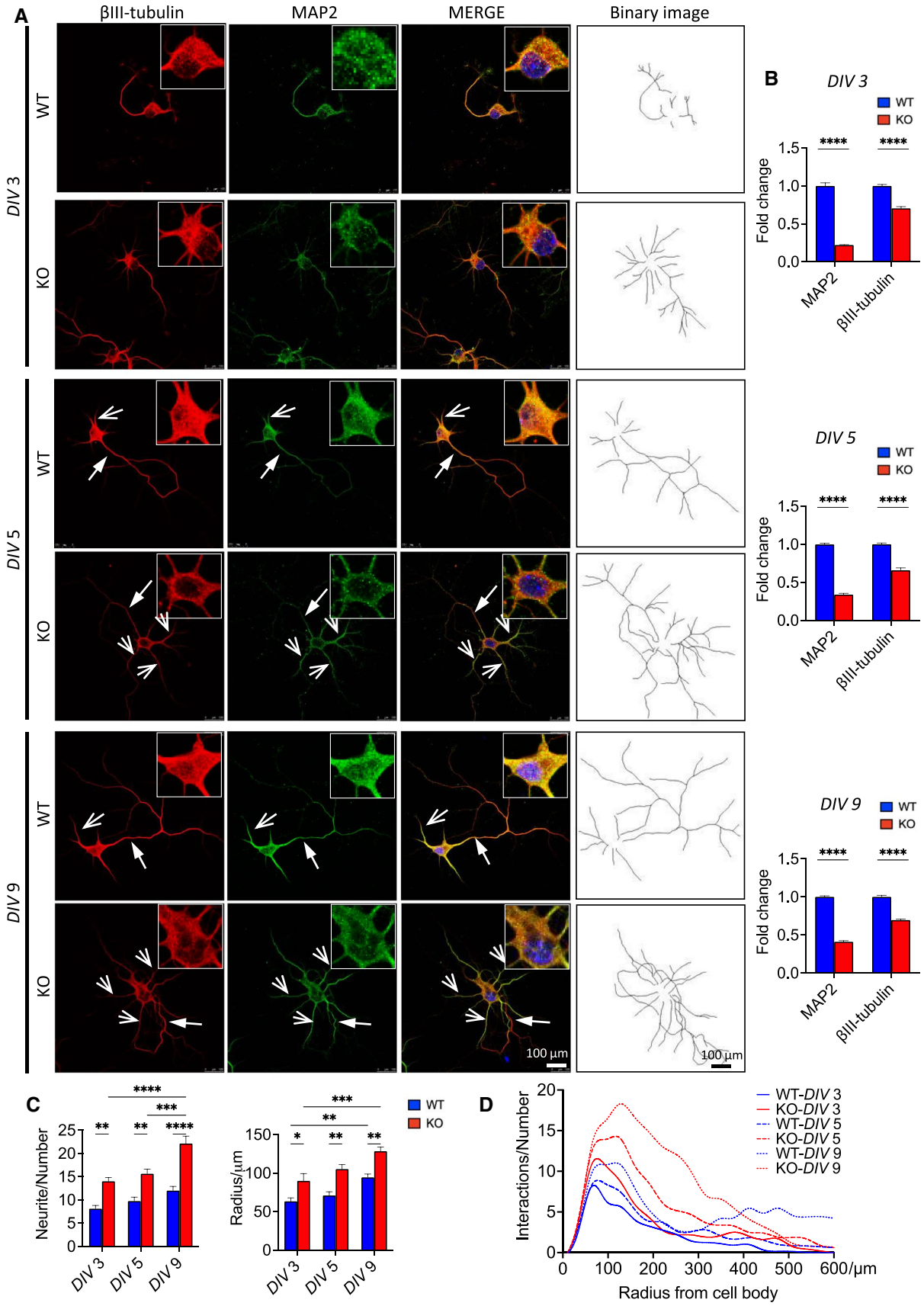
A
βIII-tubulin
MAP2
MERGE
Binary image
DIV 3
DIV 5
DIV 9
WT
KO
100 μm
B
DIV 3
DIV 5
DIV 9
WT
KO
Fold change
MAP2
βIII-tubulin
****
C
Neurite/Number
Radius/μm
DIV 3
DIV 5
DIV 9
D
Interactions/Number
Radius from cell body
WT-DIV 3
KO-DIV 3
WT-DIV 5
KO-DIV 5
WT-DIV 9
KO-DIV 9

◂**Fig. 2** Morphological differences between *Fkbp51* KO and WT primary cultured neurons. **A** Neurons were labeled with βIII-tubulin for whole neurons (red), MAP2 for soma and dendrites (green), and DAPI for nuclei (blue). Primary cultured neurons were analyzed at *DIV*3, *DIV*5, and *DIV*9. Solid head arrows indicate axon outgrowth, while line head arrows indicate dendrite outgrowth. Inset of each image showed the magnified staining of soma area. Scale bar = 100 μm. **B** Quantification of MAP2 and βIII-tubulin labelling in primary cultured hippocampal neurons. **C**, **D** Statistical analyses of neurite numbers, radius of maximum intersections and intersections at different radii in treated and untreated WT and *Fkbp51* KO neurons. *DIV*: days in vitro. Data represent mean ± SEM of 8–10 neurons from 3 independent experiments. *P* value shown in **B** was determined by Student's unpaired *t*-test, and *P* values shown in **C** and **D** were determined by two-way ANOVA. $*P < 0.05$; $**P < 0.01$; $***P < 0.001$; $****P < 0.0001$. Immunofluorescence labeling of βIII-tubulin, F-actin, and Tau is included in the Supplementary Information, SI-Fig. 2

## FKBP51 affects Parkin expression and stability and is involved in Parkin ubiquitin-mediated degradation

The effect of *Fkbp51* knockdown on Parkin expression in vitro was performed in an attempt to experimentally test the relationship between Parkin and FKBP51. Utilizing the human neuroblastoma cell line SH-SY5Y, we studied the effect of siRNA knockdown of *Fkbp51* on Parkin expression levels and cellular morphology. Compared to the scramble siRNA control, *Fkbp51* siRNA treatment reduced the IF signal intensity of MAP2 and Tau. Additionally, we observed that a higher intensity of F-actin labeling shifted from the soma to the dendrites when comparing the *Fkbp51* siRNA group and control, with a significant increase in the Parkin signal in the perinuclear area. Importantly, the *Fkbp51* siRNA treatment group also exhibited altered morphology, with an increase from two to many neurite outgrowths, a result akin to the neuron morphological alterations seen in *Fkbp51* KO (Fig. 6A). Western blotting analysis confirmed a reduction in FKBP51 protein and an increase in Parkin levels in *Fkbp51* siRNA-treated SH-SY5Y cells compared to scrambled siRNA treated cells (Fig. 6B). Thus, *Fkbp51* siRNA altered microtubule-associated protein expression and cellular morphology.

As an E3 ubiquitin ligase, Parkin mediates the targeting of protein degradation machinery. Proper regulation of Parkin is critical, either via degradation or transitioning between active and inactive conformations [12]. We performed in vitro overexpression experiments to test whether FKBP51 regulates Parkin expression. The Flag-*Fkbp51* plasmid was transfected into cells. Following FKBP51 overexpression, endogenous Parkin expression was dramatically decreased in a dose-dependent manner (Fig. 6C). This finding suggests that FKBP51 expression reduces Parkin expression, potentially by affecting Parkin stability. To investigate this possibility, cells were transfected with Flag-*Fkbp51* prior to the addition of cycloheximide (CHX), a protein synthesis inhibitor. The cells were harvested at 2, 4, 12, and 24 h post-CHX treatment, and Parkin protein levels were examined. Following CHX treatment, Parkin protein levels declined steadily in Flag-*Fkbp51*-treated cells (Fig. 6D), suggesting that FKBP51 directly diminishes Parkin stability and plays a role in Parkin self-degradation.

To study the role of ubiquitin in this process, His-Parkin, Flag-*Fkbp51*, and HA-ubiquitin were co-transfected in different combinations. As shown in Fig. 6E, compared to His-Parkin expression alone (Fig. 6E, lane 1), co-transfection of both Parkin and ubiquitin (HA-UB) resulted in diminished Parkin levels (Fig. 6E, lane 2). Intriguingly, decreased endogenous FKBP51 expression was also observed (Fig. 6E, lane 2). The data indicate ubiquitin-mediated Parkin and FKBP51 degradation. As expected, co-transfection of FKBP51 and His-Parkin without ubiquitin resulted in a significant decrease in Parkin expression relative to that of cells transfected with His-Parkin alone (Fig. 6E, lane 3 vs lane 1) demonstrating that overexpression of FKBP51 reduces Parkin. Co-transfection of ubiquitin with FKBP51 and Parkin dramatically reduced endogenous FKBP51, Flag-FKBP51, and Parkin expression (Fig. 6E, lane 4), suggesting that ubiquitin enhances FKBP51 activity. The bottom panel is the full gel blot for HA-UB. Taken together, these results indicate that FKBP51 regulates Parkin protein level in a dose- and ubiquitin-mediated manner. Next, the direct interaction between the Parkin and FKBP51 proteins was investigated using co-IP.

It has been reported that FKBP51 can interact with neuronal MAPs, Tau, and Tubulin [10, 42], but the possibility that FKBP51 interacts directly with Parkin has not been previously investigated. To further explore the interactions among FKBP51, Parkin, βIII-tubulin, and Tau, co-IP experiments were performed in SH-SY5Y cells. As shown in Fig. 6F, FKBP51 precipitated with βIII-tubulin and Tau, confirming previous findings. FKBP51 also precipitated with Parkin, demonstrating a probable interaction. Furthermore, evidence was found that suggests Parkin precipitates with MAP2 (Fig. 6F), supporting previous research that indicated the possible association of these two proteins [63]. We conclude that FKBP51 interacts with each of these proteins, but whether directly or indirectly requires further determination.

Some Parkin phosphorylation sites are essential for its activation and disease onset [44, 66]. We further investigated a functional site at Ser65 of Parkin and its role in FKBP51 interaction (Fig. 6G). Relative to His-Parkin alone, when Flag-*Fkbp51* was co-transfected (lane 3), the Parkin protein level decreased in a manner consistent with our previous observations. When mutated His-Parkin Ser65Ala (S65A) was co-transfected with Flag-Fkbp51 (lane 4), Parkin protein was not decreased. The data suggests that Parkin Ser65 is a critical site for Parkin and FKBP51 interaction.

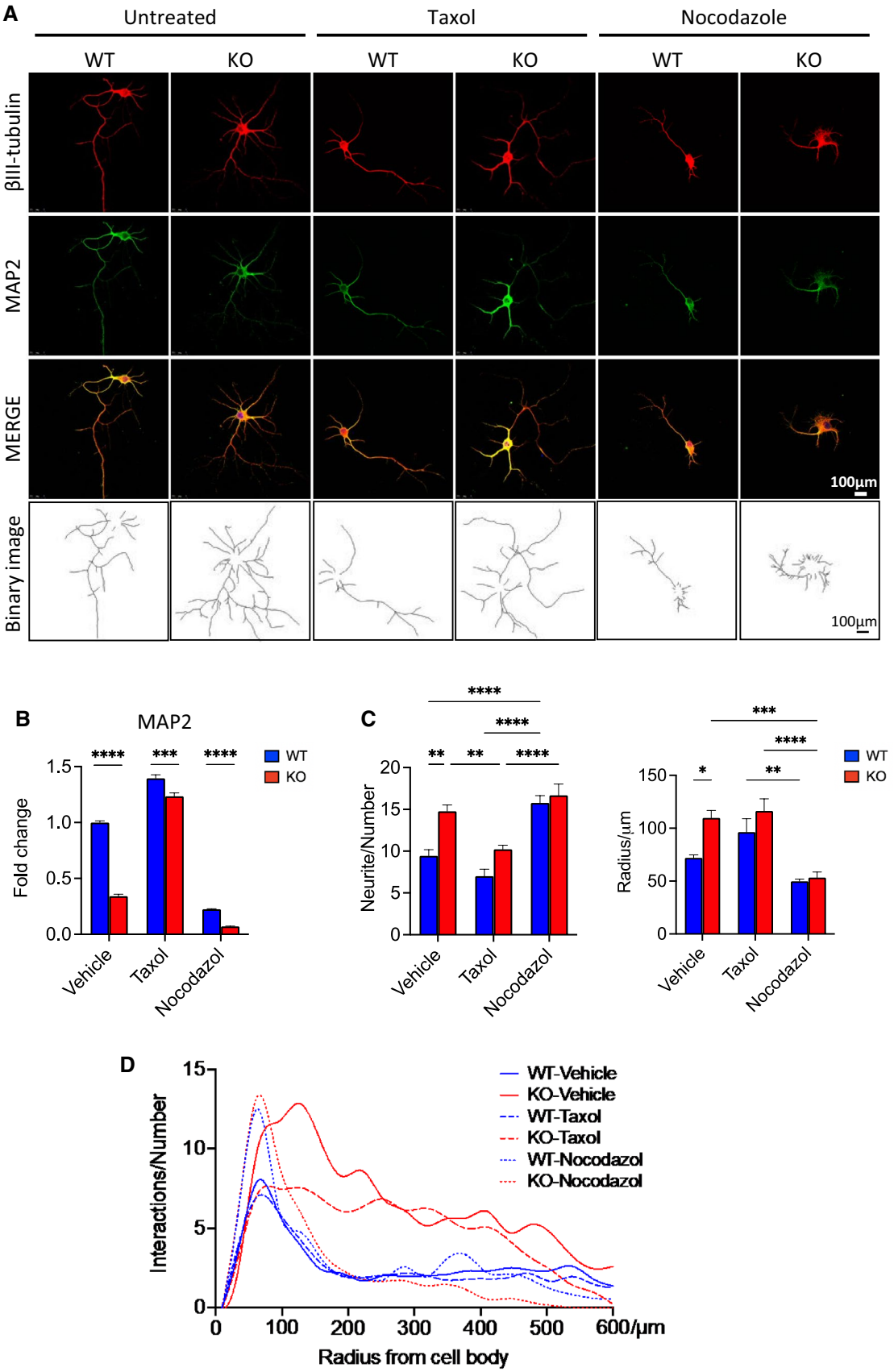
A
Untreated
Taxol
Nocodazole
WT
KO
WT
KO
WT
KO
βIII-tubulin
MAP2
MERGE
Binary image
100μm
100μm
B
MAP2
Fold change
WT
KO
Vehicle
Taxol
Nocodazol
C
Neurite/Number
Radius/μm
D
Interactions/Number
Radius from cell body
WT-Vehicle
KO-Vehicle
WT-Taxol
KO-Taxol
WT-Nocodazol
KO-Nocodazol

◂**Fig. 3** *Fkbp51* KO neuronal polarization sensitive to microtubule stability alteration. **A** Morphological differences between *Fkbp51* KO and WT primary cultured neurons are observable at *DIV 9*. Neurons are labeled with βIII-tubulin (red) and MAP2 (green). Hippocampal neurons from *Fkbp51* KO mice exhibit enhanced neurite outgrowth. Taxol reduced dendrite outgrowth from *Fkbp51* KO neurons, while nocodazole reduced minor neurite formation in both WT and *Fkbp51* KO, with more obvious neuronal deformation present in *Fkbp51* KO. Scale bar = 100 µm. **B** Quantification of the MAP2 labeling in primary cultured hippocampal neurons. **C**, **D** Statistical analyses of neurite numbers, radius of maximum intersections and intersections at different radii in treated and untreated WT and *Fkbp51* KO neurons. Data represent mean ± SEM of 8 ~ 10 neurons from 3 independent experiments. *P* value shown in **B** was determined by Student's unpaired *t*-test, and *P* values shown in **C**, **D** were determined by two-way ANOVA. **P* < 0.05; ***P* < 0.01; ****P* < 0.001; *****P* < 0.0001

## Discussion

Herein we report that *Fkbp51* impacts neuronal morphology and regulates Parkin protein level. We demonstrated alterations of hippocampus size by measuring hippocampal and DG dimensions in male *Fkbp51* KO and WT mice. Application of AI tools significantly advanced our understanding of these morphological changes in a more detailed fashion, increased the sensitivity of measurements, and allowed us to identify the differences between male KO and WT as well as between right and left hemispheres. We reported that microtubule-associated protein changes in *Fkbp51* KO mice may be implicated in dendritic outgrowth. Pharmacological manipulations supported the notion that *Fkbp51* regulates microtubule dynamics. Further investigation found that deletion of *Fkbp51* resulted in no obvious alterations in microtubule-associated mRNA expression but significant changes in the expression of several proteins, including decreases in βIII-tubulin, MAP2, and Tau, and a more than doubling of Parkin. Consistently, previous studies have demonstrated reduced expression of Tau in *Fkbp51* KO [6], 7. We focused our investigation on FKBP51 and Parkin to provide a mechanistic understanding of the FKBP51 and Parkin interaction by either overexpression or siRNA knockdown of *Fkbp51*, revealing an inverse relationship between FKBP51 and Parkin protein levels. Co-transfection experiments identified a dose-dependent and ubiquitin-mediated negative correlation between FKBP51 and Parkin protein levels. Moreover, co-IP experiments confirmed that FKBP51 binds βIII-tubulin, Tau, and Parkin. Finally, we demonstrated that the Parkin amino acid residue Ser65 is a critical site for FKBP51 and Parkin interaction. Our discovery of the role of *Fkbp51* in neuronal development via regulation of Parkin is novel and its role in the regulation of MAP2 and Tubulin levels during neuronal polarization may be the key for advancing future research on their associations with disease onset.

There are known genetic determinants of hippocampus volume and its association with mental illness [2, 29, 48, 54, 94]. Previous literature demonstrates that FKBP51 is critical for neuronal development and stress-related psychiatric diseases [40, 42]. For example, *Fkbp51* has been associated with depression, PTSD, and other psychiatric disorders, and PTSD patients display hippocampal volume changes [21, 80, 84]. Thus, our KO model represents a genetically relevant in vivo model for identifying the long-term effects of neurological and morphological alterations. Hippocampal CA and DG volumes are smaller in MDD patients, however, exposure to early life stress results in increased volume, and more interestingly, alleles within the *FKBP51* gene are associated with different responses to treatment of those patients with early life stress. Additionally, *FKBP51* haplotype was shown to modulate the resting brain activity of parents who lost their only child [38, 46, 55]. These data suggest that hippocampal volume is at least partially determined by FKBP51 genetics. Distinct genotypes respond differently to treatment, indicating a role for FKBP51 in gene-environment interaction. Furthermore, FKBP51 does play a role in neuronal plasticity and brain activity [22]. Indeed, we also observe alterations in synaptic plasticity in *Fkbp51* KO mice [58]. The breadth of these profound findings suggests an extensive role for FKBP51 in normal biological function and in disease onset. However, a full mechanistic understanding of its modes of action in humans is missing critical details.

*FKBP51* genotype-dependent increases in coupling between the left amygdala and left hippocampus suggest its role in emotional processing and differences between hemispheres [30]. Another study found a positive correlation between the severity of repression and left hippocampal volume in a subgroup of PTSD with a specific *FKBP51* genotype [92]. Interestingly, glucocorticoid receptor (GR), a protein that forms a complex with FKBP51 to carry out its function, has a "protective" genotype that responds to emotional trauma and affects the reductions in left hippocampal volumes [41]. In our study, the AI tool enabled a more accurate quantification of morphological changes in the male mouse hippocampus. In addition to the genotype-specific differences, the differences between left and right hemispheres were also quite interesting. Thus, our *Fkbp51* KO model supports the notion that the absence of FKBP51 produces alterations in hippocampal morphology, the degree of which may be hemisphere-specific.

The hippocampus plays key roles in spatial navigation and episodic memory, and segments along the transverse axis of the hippocampal pyramidal cell layer reflect their morphological and functional differences [19, 71]. Previous research determined that these layers may possess differences in circuit function and activity, particularly differences between deep and superficial neurons correlated with physiological functions and connections to basket cells [71], [73]. In our study, we have identified a role for FKBP51 in neuronal development via the post-translational regulation

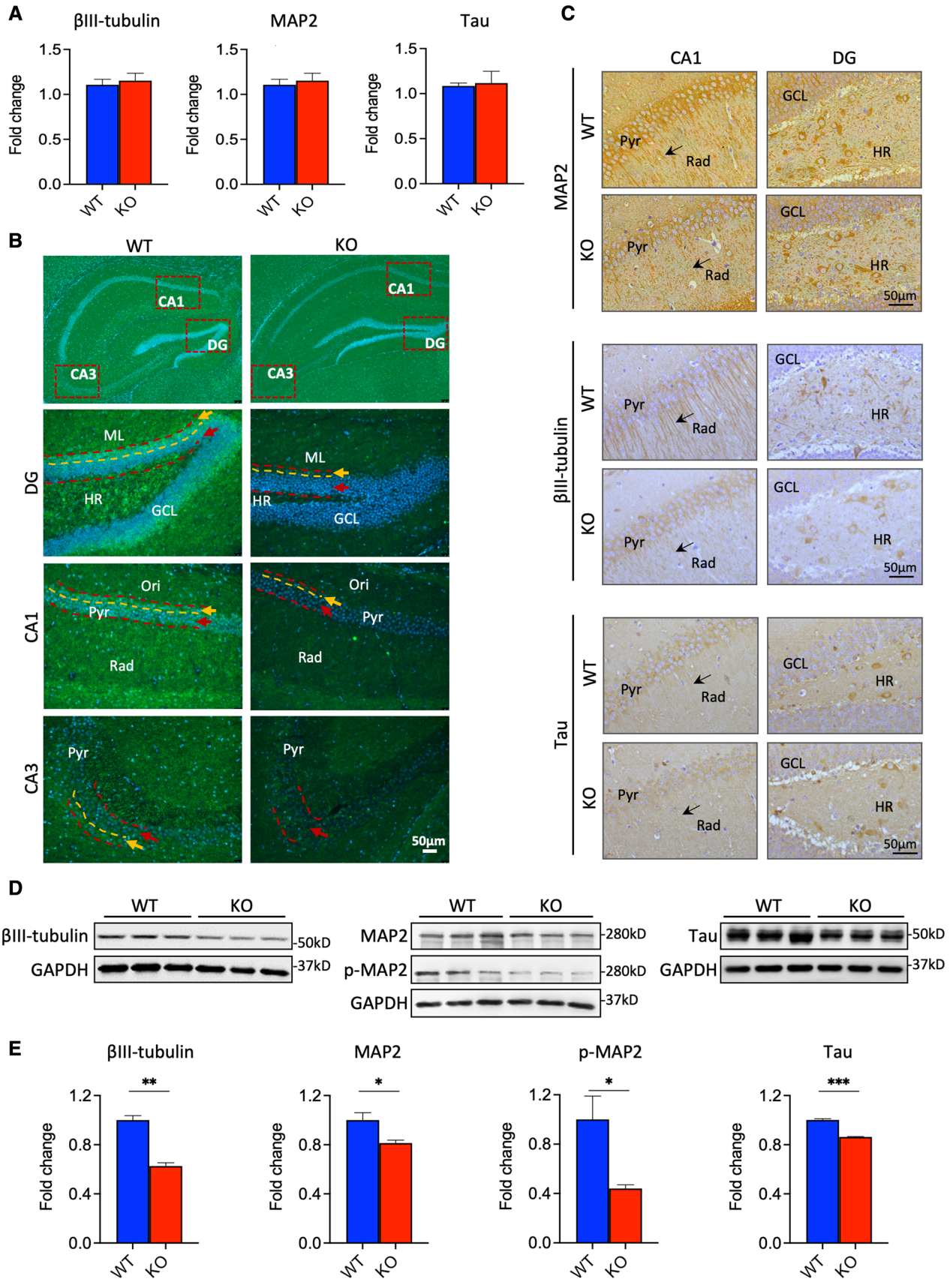
A
βIII-tubulin
MAP2
Tau
Fold change
1.5
1.0
0.5
0.0
WT
KO
B
WT
KO
CA1
DG
CA3
ML
HR
GCL
Ori
Pyr
Rad
50μm
C
CA1
DG
MAP2
βIII-tubulin
Tau
WT
KO
GCL
HR
Pyr
Rad
50μm
D
βIII-tubulin
GAPDH
MAP2
p-MAP2
Tau
50kD
37kD
280kD
E
βIII-tubulin
MAP2
p-MAP2
Tau
Fold change
1.2
0.8
0.4
0.0
**
*
***

◂**Fig. 4** In vivo differences in βIII-tubulin, MAP2, and Tau expression in the hippocampus. **A** No significant differences were found in the expression levels of *Tubb3*, *Map2*, or *Tau* mRNA. **B** MAP2 and DAPI immunofluorescent labeling of hippocampus and magnified subfields including DG, CA1, and CA3. **C** In the CA1 and DG hippocampal subfields, MAP2 and βIII-tubulin expression are significantly lower in the *Fkbp51* KO than in the WT, particularly in the Rad. Tau protein expression levels are also lower in the *Fkbp51* KO than in the WT (scale bar = 50 μm). **D** Western blotting confirmed the reduced expression of the MAP2, p-MAP2, βIII-tubulin, and Tau proteins. **E** Quantification of the MAP2, p-MAP2, βIII-tubulin and Tau proteins in the hippocampus. Data represent the mean ± SEM normalized to GAPDH. Pyr, pyramidal cell layer; Rad, radiatum layer; HR, hilar region; GCL, granule cell layer. Data represent mean ± SEM of 6 mice per genotype. *P* values were determined by Student's unpaired *t*-test. $^{*}P < 0.05$; $^{**}P < 0.01$; $^{***}P < 0.001$

of microtubule associated protein expression (i.e., down regulation of MAP2, and upregulation of Parkin). MAP2 labeling in vitro and in vivo revealed that changes in expression levels were consistent. Particularly striking were MAP2 labeling differences in the deep cell layer of GCL of DG, as well as deep pyramidal neurons of CA1 and CA3. Clearly, *Fkbp51* KO produces changes in neuronal development and hippocampal morphology.

Microtubules are essential for neuronal development and interact with microtubule-associated proteins (MAPs), Tau, and Parkin [63]. Mutations and variations in these proteins are associated with major neurodevelopmental and neurodegenerative diseases, such as Parkinson's Disease (PD) and Alzheimer's disease (AD) [8, 15, 26, 43, 75]. Recent research has established that Parkin, a multifunctional ubiquitin ligase, binds and stabilizes microtubules, regulates gene expression, and participates in mitochondrial homeostasis [18, 63, 82, 88]. Parkin can also directly form Tubulin dimers via ubiquitination and through interactions with hallmark proteins of AD [52, 63]. Parkin absence accelerates microtubule aging in dopaminergic neurons [9, 62]. Interestingly, FKBP51 binds Tubulin and associates with MAPs, Tau, Hsp90, and other chaperones to guide neuronal differentiation [10, 59]. However, no prior studies have elucidated the relationship between FKBP51 and Parkin.

In this study, we revealed the potential interaction of these two proteins. Intuitively, if the morphological alterations that were observed in vitro persist in the whole organism, they must affect the entire neuronal organization in vivo. Greater dendrite outgrowth in the *Fkbp51* KO could alter normal neuronal function, resulting in connectivity differences. Our group and others recently found that *Fkbp51* plays a role in synaptic plasticity [5, 58]. Neuronal polarization is a dynamic process including microtubule protein transportation, cross-linking between microtubules and other proteins, as well as the internal traction force in the axon [16, 83, 86, 87]. In *Fkbp51* KO neurons, the microtubule dynamic was altered due to the downregulation of microtubule-associated protein and significant upregulation of Parkin, which stabilized the microtubules. We know that dynamic protein networks assemble on and inside the cell membrane and that microtubules forming the cytoskeleton are responsible for cell shape. Thus, Parkin and FKBP51 interaction may play a prominent role in the regulation of microtubule-related protein networks and cell morphology. It is also plausible that FKBP51 regulates the functions of other protein via its isomerase activity and its involvement in the phosphorylation, ubiquitination, and lipidation of proteins [60, 61]. Importantly, we identified that the Parkin Ser65 residue is critical for FKBP51 and Parkin interaction, and that Ser65 phosphorylation is associated with disease onset. We propose a model for their interactions based on our findings (Fig. 7). Normally, FKBP51 interacts with Parkin and participates in Parkin self-degradation, maintaining normal Parkin activity and allowing microtubule-related proteins (or substrates like Tubulin, Map2, Tau, etc.) to participate in normal degradation. In the absence of FKBP51, their interactions may result in reduced Parkin self-degradation, increasing the level of Parkin protein and enhancing Parkin activity, promoting downstream substrate degradation. We speculate that these changes produce a new homeostasis of the cytoskeletal network and function that can affect neuronal development and hippocampal formation, resulting in alterations in plasticity and connectivity [22, 59]. These changes would further explain the contribution of FKBP51 in stress-related mental illnesses [4, 85, 93].

The discovery that Parkin activity is regulated by FKBP51 opens a new strategy for the treatment of Parkin-associated neurological diseases. It is known that some forms of PD exhibit inactivated Parkin activity [35], and it has been suggested that chronic stress conferred by the metabolism of dopamine in dopaminergic neurons may render those neurons more dependent on Parkin [20]. We observed ubiquitin-mediated degradation of Parkin, which is consistent with a previous report that Parkin self-regulation could be exacerbated via ubiquitin-assisted degradation [13]. Evidence of FKBP51-dependent and ubiquitin-mediated regulation of Parkin activity and doubled Parkin protein in the hippocampus of *Fkbp51* KO mice suggests an upstream regulatory role for FKBP51 in the control of Parkin activity. Parkin has been associated with multiple diseases and functions as an E3 ligase in the ubiquitination pathway that controls protein quality and gene expression [18, 63, 82, 88]. Both FKBP51 and Parkin are involved in neuronal function and share several overlapping functions related to disease development [15, 33]. FKBP51 is implicated in stress-related disorders, including PTSD, depression, and addiction [4, 32, 36, 57], and a recent meta-analysis of GWAS found *PARK2* is an additional gene associated with PTSD [49]. Functional SNPs linked to high or low FKBP51 protein expression level in humans are associated with disease

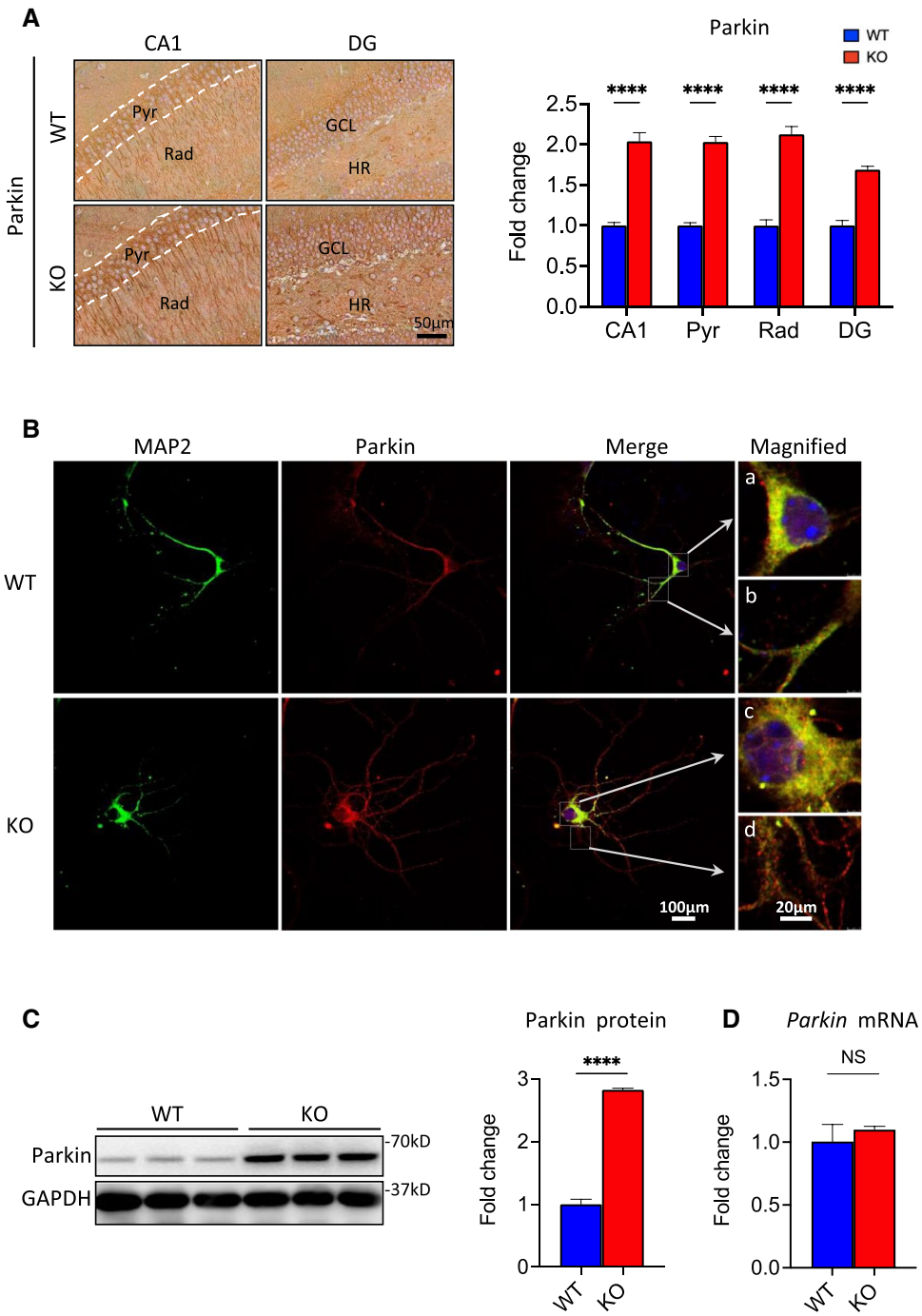


**Fig. 5** Increased Parkin levels occur in *Fkbp51* KO mice via post-translational regulation. **A** Parkin expression is significantly increased in the *Fkbp51* KO in the hippocampal subregions CA1 and DG, scale bar = 50 µm. **B** Primary cultured WT and *Fkbp51* KO hippocampal neurons labeled at *DIV*9 with MAP2 (green), Parkin (red), and DAPI (blue), scale bar = 100 µm. WT neurons express more MAP2 but less Parkin than *Fkbp51* KO neurons in the soma and dendrites. The magnified panel highlights the distinct labeling patterns in WT and *Fkbp51* KO soma and dendrites. **C** Western blotting confirms significantly higher Parkin protein expression in the *Fkbp51* KO hippocampus. Quantification of the western blot density indicates that the Parkin protein is significantly elevated in the *Fkbp51* KO hippocampus (over 2.5-fold). **D** No significant differences were found in *Park2* mRNA expression. Data represent the mean ± SEM normalized to GAPDH. Pyr, pyramidal cell layer; Rad, radiatum layer; HR, hilar region; GCL, granule cell layer. Data represent mean ± SEM of 6 mice per genotype. *P* values were determined by Student's unpaired *t*-test. ****$P < 0.0001$

onset and response to traumatic events. A humanized mouse model further supports functional SNPs affecting hormonal stimulation in primary cultured neurons [50]. Thus, fine tuning FKBP51 protein activity could alter its interactions with associated proteins and regulate the function of downstream targets. Given its role in altering cell morphology, its role in the regulation of the neuronal cytoskeleton and neuron function are exciting avenues of research.

In summary, this research identified a novel function of FKBP51 as a determinant of neuronal development and hippocampal morphology in male mice. The mechanism may be related to its role in the post-translational regulation of microtubule-related protein expression, through which it directly influences Parkin function and activity. These findings provide a foundation for further studies on the role of FKBP51 in neuronal function and disease development and may aid in understanding the value of FKBP51 as a genetic

factor for depression, PTSD, and other mental illnesses. Revealing these novel functions of FKBP51 may lead to the development of rational pharmacological interventions.

## Materials and methods

### Animals

All experimental protocols were reviewed and approved by the Animal Care and Research Advisory Committee of the Institute of Laboratory Animal Sciences at the Chinese Academy of Medical Sciences and the Indiana University School of Medicine. The animals were maintained in facilities fully accredited by the Association for the Assessment and Accreditation of Laboratory Animal Care (AAALAC). The development of *Fkbp51* KO mice was described in a previous publication [91].

### H&E staining and measurement of hippocampal morphology

Brain sections from adult *Fkbp51* KO and WT animals were analyzed for anatomical differences. Coronal brain sections from a total of 10 male mice (5 *Fkbp51* KO mice and 5 WT controls) at 8 weeks of age were obtained. The whole brains were fixed in 4% paraformaldehyde, embedded in paraffin, and serially sectioned at a thickness of 4 µm. Sections from both 5 KO ($N=135$ sections) and 5 WT ($N=152$ sections) mice near Bregma − 2.18 mm were collected for image analysis. H&E staining was applied as previously described [91]. The architecture of the hippocampus was observed on sections corresponding to the same anatomical plane using a light microscope and camera (Leica CTR6000 with DFC450 C, Wetzlar, Germany).

### AI-assisted morphological analysis

Machine learning was applied to accurately assess hippocampal morphology. A total of 287 stacks of coronal view images from of 5 WT and 5 *Fkbp51*-KO mouse brains were analyzed. Each image in a stack was processed separately. The 2D hippocampus interface was first segmented at each stack depth, and the centerline of the segmented regions was approximated to obtain two curves, one for CA and one for DG. Based on the local characteristics (position and curvature) of each curve, contextual landmarks of interest were located, upon which 2D shape features describing the hippocampus were calculated. To tackle the spatially varying contrast and color/intensity statistics throughout the images, a local, adaptive approach was followed. Each image was preprocessed in grayscale with the locally adaptive histogram equalization method for contrast enhancement, as previously described [95]. The hybrid probability-driven deformable model was applied as established prior [78]. For initial training of the region classification component of the method, ~ 200 random samples (small regions) of the interface of interest and another ~ 200 samples from the surrounding regions, from all (~ 30) images of four stacks (two WT and two KO) were manually obtained. For each examined image, after the initial probability field was obtained, the evolution of the deformable region produced more samples for the positive and negative hypotheses (desired interface and surroundings, respectively). The embedded classifier was thus continually re-trained and the image probability field was updated throughout the model evolution, incorporating local image statistics using the published method [78]. The final segmentation results did show some inaccuracies, primarily at image regions with a high degree of intensity ambiguity. It is worth noting that the semi-automatic graph cuts were also tested with acceptable results, but required manual region annotation as well [65].

### Primary hippocampal neuron culture and immunofluorescence

Primary cultures of hippocampal neurons were prepared from the hippocampi of mouse embryos at embryonic day 15.5 (E15.5) as previously described, with some modifications [56]. For the drug treatment groups, Taxol (Millipore, Billerica, MA, USA) or nocodazole (Millipore, Billerica, MA, USA) was added to culture medium at final concentrations of 3 nM or 50 nM, respectively. DMSO was applied to the untreated group as a vehicle control. Neuronal development was assessed using IF labeling of βIII-tubulin, MAP2, and DAPI. The IF of primary cultured hippocampal neurons on day 3, 5, or 9 in vitro (*DIV* 3, 5, or 9) were evaluated for MAP2, βIII-tubulin, and DAPI, as previously described [81]. All experiments were repeated independently 3 times. The antibodies used in this study are listed in Supplementary information Table1.

### Western blotting analysis, immunohistochemistry, and quantitative real-time PCR

Proteins were isolated using radioimmunoprecipitation assay (RIPA) lysis buffer and total mRNA was isolated in TRIzol® from hippocampi (Beyotime, Jiangsu, China) ($N=3$–5). Western blotting and immunohistochemistry were performed as previously described [56]. The antibodies used are listed in SI-Table1. Reverse transcription (RT) and quantitative real-time PCR were conducted as previously described [28]. The relative mRNA expression levels were normalized to *Rpl7*, which was not differentially expressed between the *Fkbp51* KO and WT groups. The primers utilized are listed

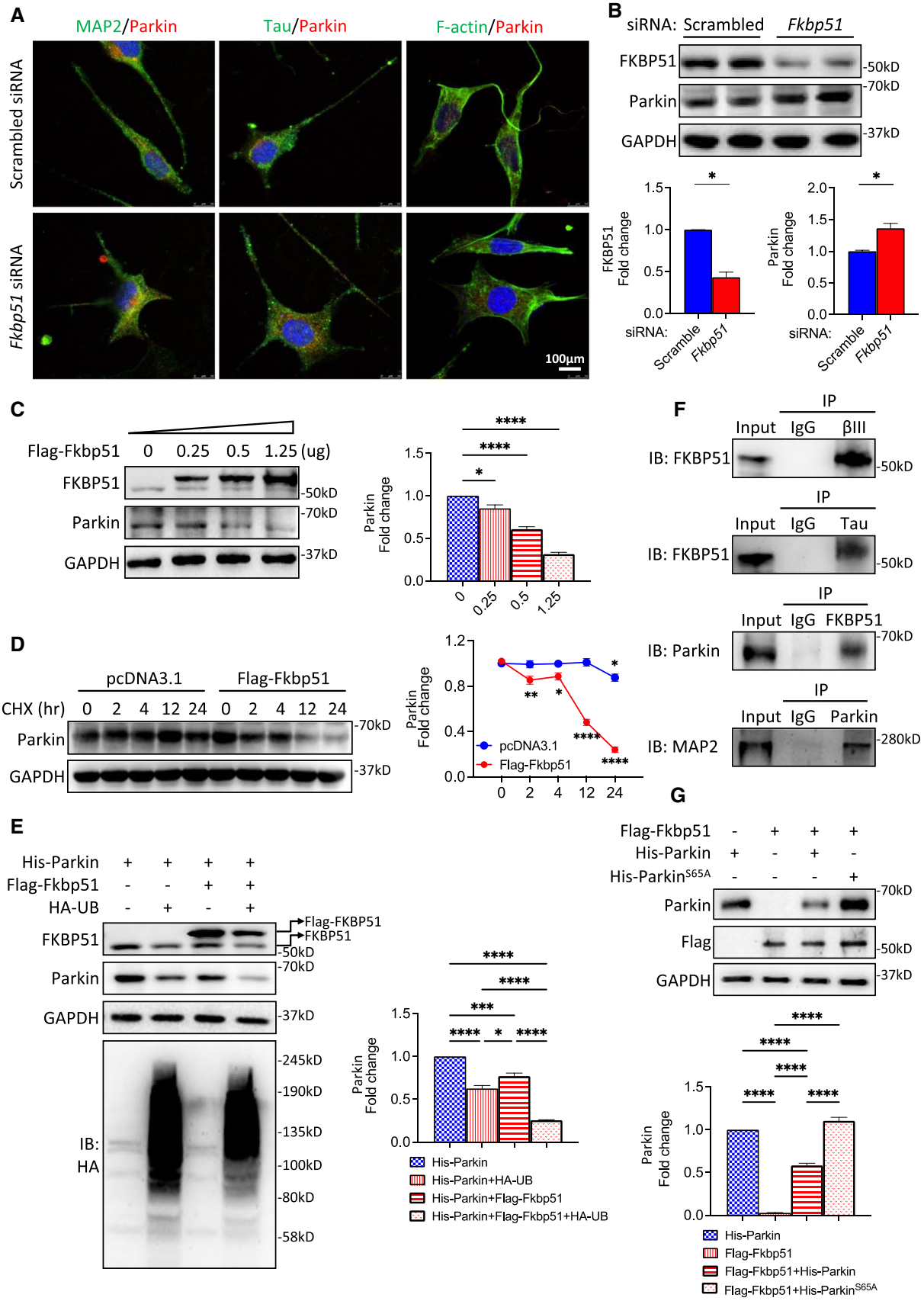
A
MAP2/Parkin
Tau/Parkin
F-actin/Parkin
Scrambled siRNA
Fkbp51 siRNA
100μm
B
siRNA: Scrambled Fkbp51
FKBP51
Parkin
GAPDH
-50kD
-70kD
-37kD
FKBP51 Fold change
Parkin Fold change
siRNA: Scramble Fkbp51
C
Flag-Fkbp51 0 0.25 0.5 1.25 (ug)
FKBP51
Parkin
GAPDH
-50kD
-70kD
-37kD
Parkin Fold change
D
pcDNA3.1
Flag-Fkbp51
CHX (hr) 0 2 4 12 24 0 2 4 12 24
Parkin
GAPDH
-70kD
-37kD
Parkin Fold change
pcDNA3.1
Flag-Fkbp51
E
His-Parkin + + + +
Flag-Fkbp51 - - + +
HA-UB - + - +
FKBP51
Flag-FKBP51
FKBP51
-50kD
Parkin
-70kD
GAPDH
-37kD
IB: HA
-245kD
-190kD
-135kD
-100kD
-80kD
-58kD
Parkin Fold change
His-Parkin
His-Parkin+HA-UB
His-Parkin+Flag-Fkbp51
His-Parkin+Flag-Fkbp51+HA-UB
F
IP
Input IgG βIII
IB: FKBP51
-50kD
Input IgG Tau
IB: FKBP51
-50kD
Input IgG FKBP51
IB: Parkin
-70kD
Input IgG Parkin
IB: MAP2
-280kD
G
Flag-Fkbp51 - + + +
His-Parkin + - + -
His-Parkin$^{S65A}$ - - - +
Parkin
Flag
GAPDH
-70kD
-50kD
-37kD
Parkin Fold change
His-Parkin
Flag-Fkbp51
Flag-Fkbp51+His-Parkin
Flag-Fkbp51+His-Parkin$^{S65A}$

◂**Fig. 6** FKBP51 prevents disrupted SH-SY5Y cell morphology and is associated with ubiquitin-mediated degradation of Parkin. **A** Double labeling of MAP2/Parkin, Tau/Parkin, and F-actin/Parkin indicates that *Fkbp51* siRNA treatment increases the outgrowth of neurites in SH-SY5Y cells, decreases MAP2, Tau, and F-actin expression, and increases Parkin expression. **B** Western blotting confirms reduced FKBP51 and increased Parkin levels following *Fkbp51* siRNA treatment compared to those treated with the scramble siRNA control. **C** Increased expression of Flag-FKBP51 in SH-5YSY cells corresponds to a dose-dependent decrease in Parkin protein levels. **D** Parkin expression levels decreased with overexpression of *Fkbp51* but not pcDNA3.1 control. **E** Co-transfection of His-Parkin with ubiquitin HA-UB alone (lane 2), Flag-*Fkbp51* and His-Parkin (lane 3), or HA-UB and Flag-*Fkbp51* together (lane 4) promotes ubiquitin-dependent degradation of both FKBP51 and Parkin. **F** Co-IP assays show that FKBP51 binds Parkin, βIII-tubulin, and Tau. Parkin also binds MAP2. **G** Co-transfection of Flag-*Fkbp51* with Parkin$^{S65A}$ reveals S65A is a critical site for FKBP51 and Parkin interaction. Data represent mean ± SEM from 3 independent experiments. *P* value shown in **B** was determined by Student's unpaired *t*-test, *P* values shown in **C**, **E** and **G** were determined by One-way ANOVA, and *P* values shown in **D** were determined by Two-way ANOVA. *$P < 0.05$; **, $P < 0.01$; ***, $P < 0.001$; ****, $P < 0.0001$

in SI—Table 2. All experiments were repeated independently 3–5 times.

## Co-IP, Parkin stability, and Parkin mutation co-transfection

The human neuroblastoma cell lines SH-SY5Y were cultured with DMEM containing 10% FBS, 1% penicillin and streptomycin, and 2 mM GlutaMax in a humidified 37 °C incubator with 5% $CO_2$. The cells were transfected with the Flag-*Fkbp51* (HG11487-CF, Sino Biological, Beijing, China), His-*Park2* (HG12092-NH, Sino Biological, Beijing, China) or HA-ubiquitin (#18712, Addgene, Cambridge, MA, USA) plasmid for overexpression or with the human *Fkbp51* siRNA (sc-35380, Santa Cruz Biotech, Inc., Dallas, TX, USA) for knock-down, using Lipofectamine 3000 (L3000008, Life Technologies, Gaithersburg, MD, USA) according to the manufacturer's recommendations. Thirty-six hours after transfection, the cells were used for co-IP experiments. A co-IP kit (#26149, Life Technologies, Gaithersburg, MD, USA) was utilized according to the manufacturer's instructions. The Parkin S65A mutation (Parkin$^{S65A}$) was generated using the Fast Mutagenesis System (# FM111-01, TransGen Biotech Co, Beijing, China). All experiments were repeated independently 3–5 times. The antibodies used in this study are listed in Supplementary information (SI—Table 1).

For the Parkin stability study, SH-SY5Y cells were transfected with Flag-*Fkbp51* or the control plasmid and treated with CHX (2 μg/ml) to inhibit further protein synthesis after 12 h of transfection. The cells were harvested in RIPA buffer 15, 30, 45, or 60 min after CHX treatment. Aliquots of 100 μg of total protein were analyzed by western blotting.

## Sholl analysis

Sholl analysis was performed using Fiji *Image J* software [68]. First, Images were converted to a maximum intensity projection image by the NeuronJ plugin [45]. The number of primary branches, the radius of maximum intersections for the branches, and the maximum number of intersections in each radius was calculated in each generated binary image by the Simple Neurite Tracer plugin [23]. Plots were generated and statistical analysis was performed using GraphPad Prism (GraphPad Software Inc., San Diego, CA, USA).

## Statistical analysis

All values are presented as the mean ± the standard error of the mean (SEM). Student's t-test was used for comparisons between two groups, while one-way analysis of variance (ANOVA) and two-way ANOVA was performed to compare multiple group differences, followed by a Student–Newman–Keuls test for multiple comparisons. GraphPad Prism was used for data analysis (GraphPad Software Inc., San Diego, CA, USA), and significance was determined as $P < 0.05$.

**Supplementary Information** The online version contains supplementary material available at https://doi.org/10.1007/s00018-022-04167-8.

**Acknowledgements** We would also like to express our appreciation to Indiana Alcohol Research Center and Dr. Weinian Shou for the support in initiating this long-term project.

**Author contributions** Authors contributed to the study conception and design: WY, TL, YM, and GT. Material preparation, data collection and analysis were performed by BQ, ZZ, SR, YX, JW, RD, CW, KEW and GT. Data curation and formal analysis: BQ, ZZ, SR, and KEW, investigation: all authors participated. AI-assisted data analysis methodology: GT and SR. The first draft of the manuscript was written by BQ, TL, and WY and all authors commented on previous versions of the manuscript. All authors read and approved the final manuscript. Funding acquisition: WY and TL.

**Funding** This research was supported by grants from Institute of Integrative Artificial Intelligence (iAI) seed funding—IUPUI, CAMS Innovation Fund for Medical Sciences (CIFMS) (2017-I2M-3-015) and the National Science Foundation of China (nos. 81700751 and 2013CB945001).

**Availability of data and materials** All data will be available for the public after publication. No large data set needs to be deposited into the public repository.

## Declarations

**Conflict of interest** All authors have no conflicts of interest to declare.

**Ethical approval and consent to participate** Animal studies have been reviewed and approved by the Animal Care and Research Advisory Committee of the Institute of Laboratory Animal Sciences at the Chi-

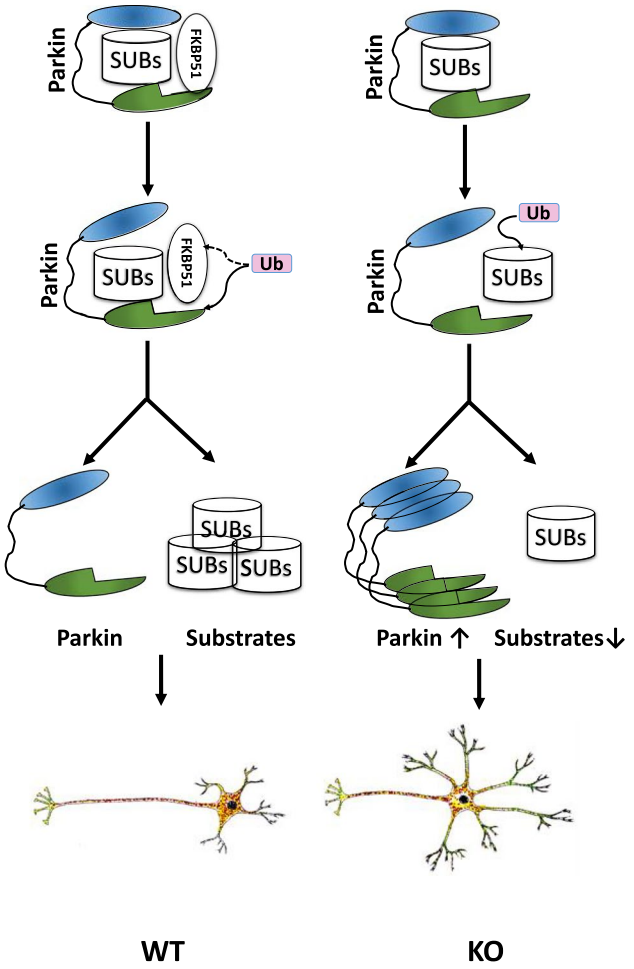


**Fig. 7** Model of morphological and molecular alterations in WT and *Fkbp51* KO neuron polarization. A schematic model demonstrating the morphological differences between WT and *Fkbp51* KO neurons, with shorter axons and greater dendritic outgrowth in *Fkbp51* KO neurons. The underlying mechanism could be due to *Fkbp51* inhibition of Parkin activity. In WT neurons, FKBP51 interacts with Parkin and regulates Parkin activity, including its ubiquitination activity, resulting in normal substrate degradation. The loss of FKBP51 interrupts the regular FKBP51 inhibition of Parkin, and may also reduce Parkin self -degradation, resulting in enhanced Parkin accumulation and enhanced Parkin activity, thus enhanced substrate degradation

nese Academy of Medical Sciences and the Indiana University School of Medicine. No human samples were included in this study.

**Consent for publication** All authors reviewed and agreed to publish the current finding.

## References


1. Arlt S, Demiralay C, Tharun B, Geisel O, Storm N, Eichenlaub M, Lehmbeck JT, Wiedemann K, Leuenberger B, Jahn H (2013) Genetic risk factors for depression in Alzheimer's disease patients. Curr Alzheimer Res 10:72–81
2. Ashbrook DG, Williams RW, Lu L, Stein JL, Hibar DP, Nichols TE, Medland SE, Thompson PM, Hager R (2014) Joint genetic analysis of hippocampal size in mouse and human identifies a novel gene linked to neurodegenerative disease. BMC Genom 15:850
3. Barnes AP, Polleux F (2009) Establishment of axon-dendrite polarity in developing neurons. Annu Rev Neurosci 32:347–381
4. Binder EB, Bradley RG, Liu W, Epstein MP, Deveau TC, Mercer KB, Tang Y, Gillespie CF, Heim CM, Nemeroff CB, Schwartz AC, Cubells JF, Ressler KJ (2008) Association of FKBP5 polymorphisms and childhood abuse with risk of posttraumatic stress disorder symptoms in adults. JAMA 299:1291–1305
5. Blair LJ, Criado-Marrero M, Zheng D, Wang X, Kamath S, Nordhues BA, Weeber EJ, Dickey CA (2019) The disease-associated chaperone FKBP51 impairs cognitive function by accelerating AMPA receptor recycling. eNeuro 6
6. Blair LJ, Nordhues BA, Hill SE, Scaglione KM, O'Leary JC 3rd, Fontaine SN, Breydo L, Zhang B, Li P, Wang L, Cotman C, Paulson HL, Muschol M, Uversky VN, Klengel T, Binder EB, Kayed R, Golde TE, Berchtold N, Dickey CA (2013) Accelerated neurodegeneration through chaperone-mediated oligomerization of tau. J Clin Investig 123:4158–4169
7. Blair LJ, Zhang B, Dickey CA (2013) Potential synergy between tau aggregation inhibitors and tau chaperone modulators. Alzheimers Res Ther. 5:41
8. Buee L, Bussiere T, Buee-Scherrer V, Delacourte A, Hof PR (2000) Tau protein isoforms, phosphorylation and role in neurodegenerative disorders. Brain Res Brain Res Rev 33:95–130
9. Cartelli D, Amadeo A, Calogero AM, Casagrande FVM, De Gregorio C, Gioria M, Kuzumaki N, Costa I, Sassone J, Ciammola A, Hattori N, Okano H, Goldwurm S, Roybon L, Pezzoli G, Cappelletti G (2018) Parkin absence accelerates microtubule aging in dopaminergic neurons. Neurobiol Aging 61:66–74
10. Chambraud B, Belabes H, Fontaine-Lenoir V, Fellous A, Baulieu EE (2007) The immunophilin FKBP52 specifically binds to tubulin and prevents microtubule formation. FASEB J 21:2787–2797
11. Chang YC, Nalbant P, Birkenfeld J, Chang ZF, Bokoch GM (2008) GEF-H1 couples nocodazole-induced microtubule disassembly to cell contractility via RhoA. Mol Biol Cell 19:2147–2153
12. Chaugule VK, Walden H (2016) Specificity and disease in the ubiquitin system. Biochem Soc Trans 44:212–227
13. Chew KC, Matsuda N, Saisho K, Lim GG, Chai C, Tan HM, Tanaka K, Lim KL (2011) Parkin mediates apparent E2-independent monoubiquitination in vitro and contains an intrinsic activity that catalyzes polyubiquitination. PLoS ONE 6:e19720
14. Conrad CD, Ortiz JB, Judd JM (2017) Chronic stress and hippocampal dendritic complexity: methodological and functional considerations. Physiol Behav 178:66–81
15. Corti O, Lesage S, Brice A (2011) What genetics tells us about the causes and mechanisms of Parkinson's disease. Physiol Rev 91:1161–1218
16. Courchet J, Lewis TL Jr, Lee S, Courchet V, Liou DY, Aizawa S, Polleux F (2013) Terminal axon branching is regulated by the LKB1-NUAK1 kinase pathway via presynaptic mitochondrial capture. Cell 153:1510–1525
17. Dannlowski U, Grabe HJ, Wittfeld K, Klaus J, Konrad C, Grotegerd D, Redlich R, Suslow T, Opel N, Ohrmann P, Bauer J, Zwanzger P, Laeger I, Hohoff C, Arolt V, Heindel W, Deppe M, Domschke K, Hegenscheid K, Volzke H, Stacey D, H. Meyer Zu Schwabedissen, H. Kugel, and B.T. Baune. (2015) Multimodal imaging of a tescalcin (TESC)-regulating polymorphism (rs7294919)-specific effects on hippocampal gray matter structure. Mol Psychiatry 20:398–404
18. Darios F, Corti O, Lucking CB, Hampe C, Muriel MP, Abbas N, Gu WJ, Hirsch EC, Rooney T, Ruberg M, Brice A (2003) Parkin

prevents mitochondrial swelling and cytochrome c release in mitochondria-dependent cell death. Hum Mol Genet 12:517–526
19. Eichenbaum H (2000) A cortical-hippocampal system for declarative memory. Nat Rev Neurosci 1:41–50
20. Ekholm-Reed S, Goldberg MS, Schlossmacher MG, Reed SI (2013) Parkin-dependent degradation of the F-box protein Fbw-7beta promotes neuronal survival in response to oxidative stress by stabilizing Mcl-1. Mol Cell Biol 33:3627–3643
21. Fani N, Gutman D, Tone EB, Almli L, Mercer KB, Davis J, Glover E, Jovanovic T, Bradley B, Dinov ID, Zamanyan A, Toga AW, Binder EB, Ressler KJ (2013) FKBP5 and attention bias for threat: associations with hippocampal function and shape. JAMA Psychiat 70:392–400
22. Fani N, King TZ, Shin J, Srivastava A, Brewster RC, Jovanovic T, Bradley B, Ressler KJ (2016) Structural and functional connectivity in posttraumatic stress disorder: associations with Fkbp5. Depress Anxiety 33:300–307
23. Ferreira TA, Blackman AV, Oyrer J, Jayabal S, Chung AJ, Watt AJ, Sjostrom PJ, van Meyel DJ (2014) Neuronal morphometry directly from bitmap images. Nat Methods 11:982–984
24. Gaali S, Kirschner A, Cuboni S, Hartmann J, Kozany C, Balsevich G, Namendorf C, Fernandez-Vizarra P, Sippel C, Zannas AS, Draenert R, Binder EB, Almeida OF, Ruhter G, Uhr M, Schmidt MV, Touma C, Bracher A, Hausch F (2015) Selective inhibitors of the FK506-binding protein 51 by induced fit. Nat Chem Biol 11:33–37
25. Gerritsen L, Milaneschi Y, Vinkers CH, van Hemert AM, van Velzen L, Schmaal L, Penninx BW (2017) HPA axis genes, and their interaction with childhood maltreatment, are related to cortisol levels and stress-related phenotypes. Neuropsychopharmacology 42:2446–2455
26. Goate A, Chartier-Harlin MC, Mullan M, Brown J, Crawford F, Fidani L, Giuffra L, Haynes A, Irving N, James L et al (1991) Segregation of a missense mutation in the amyloid precursor protein gene with familial Alzheimer's disease. Nature 349:704–706
27. Gomez TM, Letourneau PC (2014) Actin dynamics in growth cone motility and navigation. J Neurochem 129:221–234
28. Gu H, Cao Y, Qiu B, Zhou Z, Deng R, Chen Z, Li R, Li X, Wei Q, Xia X, Yong W (2016) Establishment and phenotypic analysis of an Mstn knockout rat. Biochem Biophys Res Commun 477:115–122
29. Hibar DP, Adams HHH, Jahanshad N, Chauhan G, Stein JL, Hofer E, Renteria ME, Bis JC, Arias-Vasquez A, Ikram MK, Desrivieres S, Vernooij MW, Abramovic L, Alhusaini S, Amin N, Andersson M, Arfanakis K, Aribisala BS, Armstrong NJ, Athanasiu L, Axelsson T, Beecham AH, Beiser A, Bernard M, Blanton SH, Bohlken MM, Boks MP, Bralten J, Brickman AM, Carmichael O, Chakravarty MM, Chen Q, Ching CRK, Chouraki V, Cuellar-Partida G, Crivello F, Den Braber A, Doan NT, Ehrlich S, Giddaluru S, Goldman AL, Gottesman RF, Grimm O, Griswold ME, Guadalupe T, Gutman BA, Hass J, Haukvik UK, Hoehn D, Holmes AJ, Hoogman M, Janowitz D, Jia T, Jorgensen KN, Karbalai N, Kasperaviciute D, Kim S, Klein M, Kraemer B, Lee PH, Liewald DCM, Lopez LM, Luciano M, Macare C, Marquand AF, Matarin M, Mather KA, Mattheisen M, McKay DR, Milaneschi Y, Munoz Maniega S, Nho K, Nugent AC, Nyquist P, Loohuis LMO, Oosterlaan J, Papmeyer M, Pirpamer L, Putz B, Ramasamy A, Richards JS, Risacher SL, Roiz-Santianez R, Rommelse N, Ropele S, Rose EJ, Royle NA, Rundek T, Samann PG, Saremi A, Satizabal CL, Schmaal L, Schork AJ, Shen L, Shin J, Shumskaya E, Smith AV, Sprooten E, Strike LT, Teumer A et al (2017) Novel genetic loci associated with hippocampal volume. Nat Commun 8:13624
30. Holz NE, Buchmann AF, Boecker R, Blomeyer D, Baumeister S, Wolf I, Rietschel M, Witt SH, Plichta MM, Meyer-Lindenberg A, Banaschewski T, Brandeis D, Laucht M (2015) Role of FKBP5 in emotion processing: results on amygdala activity, connectivity and volume. Brain Struct Funct 220:1355–1368
31. Horgusluoglu-Moloch E, Risacher SL, Crane PK, Hibar D, Thompson PM, Saykin AJ, Nho K, I. Alzheimer's Disease Neuroimaging (2019) Genome-wide association analysis of hippocampal volume identifies enrichment of neurogenesis-related pathways. Sci Rep 9:14498
32. Huang MC, Schwandt ML, Chester JA, Kirchhoff AM, Kao CF, Liang T, Tapocik JD, Ramchandani VA, George DT, Hodgkinson CA, Goldman D, Heilig M (2014) FKBP5 moderates alcohol withdrawal severity: human genetic association and functional validation in knockout mice. Neuropsychopharmacology 39:2029–2038
33. Kim JM, Lee KH, Jeon YJ, Oh JH, Jeong SY, Song IS, Kim JM, Lee DS, Kim NS (2006) Identification of genes related to Parkinson's disease using expressed sequence tags. DNA Res 13:275–286
34. Kremen WS, Prom-Wormley E, Panizzon MS, Eyler LT, Fischl B, Neale MC, Franz CE, Lyons MJ, Pacheco J, Perry ME, Stevens A, Schmitt JE, Grant MD, Seidman LJ, Thermenos HW, Tsuang MT, Eisen SA, Dale AM, Fennema-Notestine C (2010) Genetic and environmental influences on the size of specific brain regions in midlife: the VETSA MRI study. Neuroimage 49:1213–1223
35. LaVoie MJ, Ostaszewski BL, Weihofen A, Schlossmacher MG, Selkoe DJ (2005) Dopamine covalently modifies and functionally inactivates Parkin. Nat Med 11:1214–1221
36. Lekman M, Laje G, Charney D, Rush AJ, Wilson AF, Sorant AJ, Lipsky R, Wisniewski SR, Manji H, McMahon FJ, Paddock S (2008) The FKBP5-gene in depression and treatment response—an association study in the Sequenced Treatment Alternatives to Relieve Depression (STAR*D) Cohort. Biol Psychiatry 63:1103–1110
37. Letourneau PC, Ressler AH (1984) Inhibition of neurite initiation and growth by taxol. J Cell Biol 98:1355–1362
38. Levy-Gigi E, Szabo C, Kelemen O, Keri S (2013) Association among clinical response, hippocampal volume, and FKBP5 gene expression in individuals with posttraumatic stress disorder receiving cognitive behavioral therapy. Biol Psychiatry 74:793–800
39. Levy-Gigi E, Szabo C, Richter-Levin G, Keri S (2015) Reduced hippocampal volume is associated with overgeneralization of negative context in individuals with PTSD. Neuropsychology 29:151–161
40. Lieberman R, Armeli S, Scott DM, Kranzler HR, Tennen H, Covault J (2016) FKBP5 genotype interacts with early life trauma to predict heavy drinking in college students. Am J Med Genet B Neuropsychiatr Genet 171:879–887
41. Malhi GS, Das P, Outhred T, Dobson-Stone C, Irwin L, Gessler D, Bryant R, Mannie Z (2019) Effect of stress gene-by-environment interactions on hippocampal volumes and cortisol secretion in adolescent girls. Aust N Z J Psychiatry 53:316–325
42. Matosin N, Halldorsdottir T, Binder EB (2018) Understanding the molecular mechanisms underpinning gene by environment interactions in psychiatric disorders: the FKBP5 model. Biol Psychiatry 83:821–830
43. Matsumoto L, Takuma H, Tamaoka A, Kurisaki H, Date H, Tsuji S, Iwata A (2010) CpG demethylation enhances alpha-synuclein expression and affects the pathogenesis of Parkinson's disease. PLoS ONE 5:e15522
44. McWilliams TG, Barini E, Pohjolan-Pirhonen R, Brooks SP, Singh F, Burel S, Balk K, Kumar A, Montava-Garriga L, Prescott AR, Hassoun SM, Mouton-Liger F, Ball G, Hills R, Knebel A, Ulusoy A, Di Monte DA, Tamjar J, Antico O, Fears K, Smith L, Brambilla R, Palin E, Valori M, Eerola-Rautio J, Tienari P, Corti O, Dunnett SB, Ganley IG, Suomalainen A, Muqit MMK (2018)

Phosphorylation of Parkin at serine 65 is essential for its activation in vivo. Open Biol 8
45. Meijering E, Jacob M, Sarria JC, Steiner P, Hirling H, Unser M (2004) Design and validation of a tool for neurite tracing and analysis in fluorescence microscopy images. Cytometry A 58:167–176
46. Mikolas P, Tozzi L, Doolin K, Farrell C, O'Keane V, Frodl T (2019) Effects of early life adversity and FKBP5 genotype on hippocampal subfields volume in major depression. J Affect Disord 252:152–159
47. Ming GL, Song H (2005) Adult neurogenesis in the mammalian central nervous system. Annu Rev Neurosci 28:223–250
48. Na KS, Won E, Kang J, Kim A, Choi S, Kim YK, Lee MS, Ham BJ (2018) Interaction effects of oxytocin receptor gene polymorphism and depression on hippocampal volume. Psychiatry Res Neuroimaging. 282:18–23
49. Nievergelt CM, Maihofer AX, Klengel T, Atkinson EG, Chen CY, Choi KW, Coleman JRI, Dalvie S, Duncan LE, Gelernter J, Levey DF, Logue MW, Polimanti R, Provost AC, Ratanatharathorn A, Stein MB, Torres K, Aiello AE, Almli LM, Amstadter AB, Andersen SB, Andreassen OA, Arbisi PA, Ashley-Koch AE, Austin SB, Avdibegovic E, Babic D, Baekvad-Hansen M, Baker DG, Beckham JC, Bierut LJ, Bisson JI, Boks MP, Bolger EA, Borglum AD, Bradley B, Brashear M, Breen G, Bryant RA, Bustamante AC, Bybjerg-Grauholm J, Calabrese JR, Caldas-de-Almeida JM, Dale AM, Daly MJ, Daskalakis NP, Deckert J, Delahanty DL, Dennis MF, Disner SG, Domschke K, Dzubur-Kulenovic A, Erbes CR, Evans A, Farrer LA, Feeny NC, Flory JD, Forbes D, Franz CE, Galea S, Garrett ME, Gelaye B, Geuze E, Gillespie C, Uka AG, Gordon SD, Guffanti G, Hammamieh R, Harnal S, Hauser MA, Heath AC, Hemmings SMJ, Hougaard DM, Jakovljevic M, Jett M, Johnson EO, Jones I, Jovanovic T, Qin XJ, Junglen AG, Karstoft KI, Kaufman ML, Kessler RC, Khan A, Kimbrel NA, King AP, Koen N, Kranzler HR, Kremen WS, Lawford BR, Lebois LAM, Lewis CE, Linnstaedt SD, Lori A, Lugonja B, Luykx JJ, Lyons MJ, Maples-Keller J, Marmar C, Martin AR et al (2019) International meta-analysis of PTSD genome-wide association studies identifies sex- and ancestry-specific genetic risk loci. Nat Commun 10:4558
50. Nold V, Richter N, Hengerer B, Kolassa IT, Allers KA (2021) FKBP5 polymorphisms induce differential glucocorticoid responsiveness in primary CNS cells—first insights from novel humanized mice. Eur J Neurosci 53:402–415
51. O'Leary JC 3rd, Dharia S, Blair LJ, Brady S, Johnson AG, Peters M, Cheung-Flynn J, Cox MB, de Erausquin G, Weeber EJ, Jinwal UK, Dickey CA (2011) A new anti-depressive strategy for the elderly: ablation of FKBP5/FKBP51. PLoS ONE 6:e24840
52. Olah J, Vincze O, Virok D, Simon D, Bozso Z, Tokesi N, Horvath I, Hlavanda E, Kovacs J, Magyar A, Szucs M, Orosz F, Penke B, Ovadi J (2011) Interactions of pathological hallmark proteins: tubulin polymerization promoting protein/p25, beta-amyloid, and alpha-synuclein. J Biol Chem 286:34088–34100
53. Onoue T, Toda H, Nakai Y (2013) Childhood stress and depression. Nihon Shinkei Seishin Yakurigaku Zasshi 33:105–110
54. Pujol N, Mane A, Berge D, Mezquida G, Amoretti S, Perez L, Gonzalez-Pinto A, Barcones F, Cuesta MJ, Sanchez-Tomico G, Vieta E, Castro-Fornieles J, Bernardo M, Parellada M, P.E. GROUP. (2020) Influence of BDNF and MTHFR polymorphisms on hippocampal volume in first-episode psychosis. Schizophr Res 223:345–352
55. Qi R, Luo Y, Zhang L, Weng Y, Surento W, Jahanshad N, Xu Q, Yin Y, Li L, Cao Z, Thompson PM, Lu GM (2020) FKBP5 haplotypes and PTSD modulate the resting-state brain activity in Han Chinese adults who lost their only child. Transl Psychiatry 10:91
56. Qiu B, Hu S, Liu L, Chen M, Wang L, Zeng X, Zhu S (2013) CART attenuates endoplasmic reticulum stress response induced by cerebral ischemia and reperfusion through upregulating BDNF synthesis and secretion. Biochem Biophys Res Commun 436:655–659
57. Qiu B, Luczak SE, Wall TL, Kirchhoff AM, Xu Y, Eng MY, Stewart RB, Shou W, Boehm SL, Chester JA, Yong W, Liang T (2016) The FKBP5 gene affects alcohol drinking in knockout mice and is implicated in alcohol drinking in humans. Int J Mol Sci 17
58. Qiu B, Xu Y, Wang J, Liu M, Dou L, Deng R, Wang C, Williams KE, Stewart RB, Xie Z, Ren W, Zhao Z, Shou W, Liang T, Yong W (2019) Loss of FKBP5 affects neuron synaptic plasticity: an electrophysiology insight. Neuroscience 402:23–36
59. Quinta HR, Maschi D, Gomez-Sanchez C, Piwien-Pilipuk G, Galigniana MD (2010) Subcellular rearrangement of hsp90-binding immunophilins accompanies neuronal differentiation and neurite outgrowth. J Neurochem 115:716–734
60. Rein T (2020) Peptidylprolylisomerases, protein folders, or scaffolders? The example of FKBP51 and FKBP52. Bioessays e1900250
61. Rein T (2020) Post-translational modifications and stress adaptation: the paradigm of FKBP51. Biochem Soc Trans 48:441–449
62. Ren Y, Jiang H, Yang F, Nakaso K, Feng J (2009) Parkin protects dopaminergic neurons against microtubule-depolymerizing toxins by attenuating microtubule-associated protein kinase activation. J Biol Chem 284:4009–4017
63. Ren Y, Zhao J, Feng J (2003) Parkin binds to alpha/beta tubulin and increases their ubiquitination and degradation. J Neurosci 23:3316–3324
64. Renteria ME, Hansell NK, Strike LT, McMahon KL, de Zubicaray GI, Hickie IB, Thompson PM, Martin NG, Medland SE, Wright MJ (2014) Genetic architecture of subcortical brain regions: common and region-specific genetic contributions. Genes Brain Behav 13:821–830
65. Rother C, Kolmogorov V, Blake A (2004) GrabCut—interactive foreground extraction using iterated graph cuts. ACM Trans Graphics (SIGGRAPH) 23:309–314
66. Sarraf SA, Raman M, Guarani-Pereira V, Sowa ME, Huttlin EL, Gygi SP, Harper JW (2013) Landscape of the PARKIN-dependent ubiquitylome in response to mitochondrial depolarization. Nature 496:372–376
67. Schiene C, Fischer G (2000) Enzymes that catalyse the restructuring of proteins. Curr Opin Struct Biol 10:40–45
68. Schindelin J, Arganda-Carreras I, Frise E, Kaynig V, Longair M, Pietzsch T, Preibisch S, Rueden C, Saalfeld S, Schmid B, Tinevez JY, White DJ, Hartenstein V, Eliceiri K, Tomancak P, Cardona A (2012) Fiji: an open-source platform for biological-image analysis. Nat Methods 9:676–682
69. Schmidt MV, Paez-Pereda M, Holsboer F, Hausch F (2012) The prospect of FKBP51 as a drug target. ChemMedChem 7:1351–1359
70. Schmidt U, Buell DR, Ionescu IA, Gassen NC, Holsboer F, Cox MB, Novak B, Huber C, Hartmann J, Schmidt MV, Touma C, Rein T, Herrmann L (2015) A role for synapsin in FKBP51 modulation of stress responsiveness: Convergent evidence from animal and human studies. Psychoneuroendocrinology 52:43–58
71. Slomianka L, Amrein I, Knuesel I, Sorensen JC, Wolfer DP (2011) Hippocampal pyramidal cells: the reemergence of cortical lamination. Brain Struct Funct 216:301–317
72. Smith ME (2005) Bilateral hippocampal volume reduction in adults with post-traumatic stress disorder: a meta-analysis of structural MRI studies. Hippocampus 15:798–807
73. Soltesz I, Losonczy A (2018) CA1 pyramidal cell diversity enabling parallel information processing in the hippocampus. Nat Neurosci 21:484–493
74. Szymanska M, Budziszewska B, Jaworska-Feil L, Basta-Kaim A, Kubera M, Leskiewicz M, Regulska M, Lason W (2009) The effect of antidepressant drugs on the HPA axis activity,

glucocorticoid receptor level and FKBP51 concentration in prenatally stressed rats. Psychoneuroendocrinology 34:822–832
75. Takahashi K, Uchida C, Shin RW, Shimazaki K, Uchida T (2008) Prolyl isomerase, Pin1: new findings of post-translational modifications and physiological substrates in cancer, asthma and Alzheimer's disease. Cell Mol Life Sci 65:359–375
76. Tatro ET, Nguyen TB, Bousman CA, Masliah E, Grant I, Atkinson JH, Everall IP (2010) Correlation of major depressive disorder symptoms with FKBP5 but not FKBP4 expression in human immunodeficiency virus-infected individuals. J Neurovirol 16:399–404
77. Thompson PM, Hayashi KM, De Zubicaray GI, Janke AL, Rose SE, Semple J, Hong MS, Herman DH, Gravano D, Doddrell DM, Toga AW (2004) Mapping hippocampal and ventricular change in Alzheimer disease. Neuroimage 22:1754–1766
78. Tsechpenakis G, Chatzis SP (2011) Deformable probability maps: Probabilistic shape and appearance-based object segmentation. Comput Vis Image Underst 115:1157–1169
79. Wagner KV, Marinescu D, Hartmann J, Wang XD, Labermaier C, Scharf SH, Liebl C, Uhr M, Holsboer F, Muller MB, Schmidt MV (2012) Differences in FKBP51 regulation following chronic social defeat stress correlate with individual stress sensitivity: influence of paroxetine treatment. Neuropsychopharmacology 37:2797–2808
80. Wang C, Shen M, Guillaume B, Chong YS, Chen H, Fortier MV, Meaney MJ, Qiu A (2018) FKBP5 moderates the association between antenatal maternal depressive symptoms and neonatal brain morphology. Neuropsychopharmacology 43:564–570
81. Wang Y, Qiu B, Liu J, Zhu WG, Zhu S (2014) Cocaine- and amphetamine-regulated transcript facilitates the neurite outgrowth in cortical neurons after oxygen and glucose deprivation through PTN-dependent pathway. Neuroscience 277:103–110
82. Williams JA, Ni HM, Ding Y, Ding WX (2015) Parkin regulates mitophagy and mitochondrial function to protect against alcohol-induced liver injury and steatosis in mice. Am J Physiol Gastrointest Liver Physiol 309:G324-340
83. Wilson C, Gonzalez-Billault C (2015) Regulation of cytoskeletal dynamics by redox signaling and oxidative stress: implications for neuronal development and trafficking. Front Cell Neurosci 9:381
84. Xie P, Kranzler HR, Poling J, Stein MB, Anton RF, Farrer LA, Gelernter J (2010) Interaction of FKBP5 with childhood adversity on risk for post-traumatic stress disorder. Neuropsychopharmacology 35:1684–1692
85. Xing Y, Hou J, Meng Q, Yang M, Kurihara H, Tian J (2015) Novel antidepressant candidate RO-05 modulated glucocorticoid receptors activation and FKBP5 expression in chronic mild stress model in rats. Neuroscience 290:255–265
86. Xu K, Zhong G, Zhuang X (2013) Actin, spectrin, and associated proteins form a periodic cytoskeletal structure in axons. Science 339:452–456
87. Yadaw AS, Siddiq MM, Rabinovich V, Tolentino R, Hansen J, Iyengar R (2019) Dynamic balance between vesicle transport and microtubule growth enables neurite outgrowth. PLoS Comput Biol 15:e1006877
88. Yang F, Jiang Q, Zhao J, Ren Y, Sutton MD, Feng J (2005) Parkin stabilizes microtubules through strong binding mediated by three independent domains. J Biol Chem 280:17154–17162
89. Yang Y, Nishimura I, Imai Y, Takahashi R, Lu B (2003) Parkin suppresses dopaminergic neuron-selective neurotoxicity induced by Pael-R in Drosophila. Neuron 37:911–924
90. Yogev S, Cooper R, Fetter R, Horowitz M, Shen K (2016) Microtubule organization determines axonal transport dynamics. Neuron 92:449–460
91. Yong W, Yang Z, Periyasamy S, Chen H, Yucel S, Li W, Lin LY, Wolf IM, Cohn MJ, Baskin LS, Sanchez ER, Shou W (2007) Essential role for co-chaperone Fkbp52 but not Fkbp51 in androgen receptor-mediated signaling and physiology. J Biol Chem 282:5026–5036
92. Yun JY, Jin MJ, Kim S, Lee SH (2020) Stress-related cognitive style is related to volumetric change of the hippocampus and FK506 binding protein 5 polymorphism in post-traumatic stress disorder. Psychol Med 1–12
93. Zannas AS, Jia M, Hafner K, Baumert J, Wiechmann T, Pape JC, Arloth J, Kodel M, Martinelli S, Roitman M, Roh S, Haehle A, Emeny RT, Iurato S, Carrillo-Roa T, Lahti J, Raikkonen K, Eriksson JG, Drake AJ, Waldenberger M, Wahl S, Kunze S, Lucae S, Bradley B, Gieger C, Hausch F, Smith AK, Ressler KJ, Muller-Myhsok B, Ladwig KH, Rein T, Gassen NC, Binder EB (2019) Epigenetic upregulation of FKBP5 by aging and stress contributes to NF-kappaB-driven inflammation and cardiovascular risk. Proc Natl Acad Sci USA 116:11370–11379
94. Zhang T, Hou C, Zhang S, Liu S, Li Z, Gao J (2019) Lgl1 deficiency disrupts hippocampal development and impairs cognitive performance in mice. Genes Brain Behav 18:e12605
95. Zuiderveld K (1994) Contrast limited adaptive histogram equalization. In: Heckbert PS (ed) Graphic gems IV. Academic Press, New York

## Authors and Affiliations

**Bin Qiu[2,7] · Zhaohui Zhong[3] · Shawn Righter[4] · Yuxue Xu[2] · Jun Wang[2] · Ran Deng[2] · Chao Wang[2] · Kent E. Williams[5] · Yao-ying Ma[6] · Gavriil Tsechpenakis[4] · Tiebing Liang[5] · Weidong Yong[1,2]**

✉ Tiebing Liang
tliang@iu.edu

✉ Weidong Yong
wyong@iu.edu; yongwd@hotmail.com; yongwd@iu.edu

Bin Qiu
kennyqiu@live.com; bin.qiu@yale.edu

Zhaohui Zhong
zhongzhaohui@pkuph.edu.cn

Shawn Righter
gtsechpe@indiana.edu

Yuxue Xu
xuyuxue1127@126.com

Jun Wang
junwang138@sina.com

Ran Deng
598046836@qq.com

Chao Wang
1358560339@qq.com

Kent E. Williams
kew5@iu.edu

Yao-ying Ma
ym9@iu.edu

Gavriil Tsechpenakis
gtsechpe@indiana.edu

[1] Department of Surgery, Indiana University School of Medicine, Indianapolis, IN 46202, USA

[2] Institute of Laboratory Animal Science, Chinese Academy of Medical Sciences and Peking Union Medical College, Beijing 100021, China

[3] Department of General Surgery, Peking University People's Hospital, Beijing 100032, China

[4] Department of Computer and Information Science, Indiana University-Purdue University Indianapolis, Indianapolis, IN 46202, USA

[5] Department of Medicine, Indiana University School of Medicine, Indianapolis, IN 46202, USA

[6] Department of Pharmacology and Toxicology, Indiana University School of Medicine, Indianapolis, IN 46202, USA

[7] Department of Pharmacology, Yale University School of Medicine, New Haven, CT 06520, USA